Subject of this Document:	Feasibility of Detecting PWR Thermal Shield Support Degradation Using Ex-Core Neutron Noise
Type of Document:	Informal Letter Report
Authors:	F. J. Sweeney D. N. Fry
Date of Document:	July 1985

Prepared for
U.S. Nuclear Regulatory Commission
Office of Nuclear Reactor Regulation
under
DOE Interagency Agreement 40-551-75
NRC FIN NO. B0793

Prepared by
OAK RIDGE NATIONAL LABORATORY
Oak Ridge, Tennessee 37831
operated by
MARTIN MARIETTA ENERGY SYSTEMS, INC.
for the
U.S. DEPARTMENT OF ENERGY
under
Contract No. DE-AC05-84OR21400

CONTENTS

LIST OF FIGURES

LIST OF FIGURES (continued)

LIST OF FIGURES (continued)

FEASIBILITY OF DETECTING PWR THERMAL SHIELD SUPPORT DEGRADATION USING EX-CORE NEUTRON NOISE

F. J. Sweeney

D. N. Fry

EXECUTIVE SUMMARY

Utilities and reactor manufacturers supplied Oak Ridge National Laboratory (ORNL) with ex-core neutron noise data on four Combustion Engineering (CE) pressurized water reactors (PWRs). Of the four plants, two had experienced severe thermal shield support degradation, and one plant experienced loose or missing thermal shield support pins. ORNL reviewed and analyzed these data in search of systematic changes in the neutron noise which could indicate degradation of the thermal shield or its support structures.

Our studies have shown that degradation of thermal shield supports can be detected by analyzing ex-core neutron noise signatures for changes in the frequency of beam-mode and shell-mode type vibrations below 50 Hz. However, observations in plants with degraded thermal shield supports as well as results from vibrational models indicate that these frequency changes may be small (<3 Hz). We also concluded from these results that support degradation probably occurred early in plant life in the two plants with severe damage.

The above results indicate that neutron noise measurements must be made with sufficient care, statistical precision, and frequency resolution in order to detect degradation of core internals. Because such degradation may occur over either short or long time periods, periodic measurements should be made, and the results should be reviewed by personnel experienced in neutron noise analysis and interpretation.

1. BACKGROUND

Recently, the thermal shields of two Combustion Engineering (CE) PWRs (Reactor A and Reactor B) were found to have sustained severe damage as a result of flow-induced vibrations. In both plants, loose parts were generated in the primary system, and at Reactor A, damage to the core support barrel (CSB) also occurred. The thermal shields of these two plants have since been removed. At Reactor C, also a CE PWR, several pins used to support the thermal shield were found to be missing, although no damage occurred to the thermal shield or core barrel. Loose thermal shields have also occurred in three Babcock and Wilcox (B&W) PWRs (Oconee-1, -2, and -3) due to loose lower support bolts, and in a Westinghouse PWR (Trino).

In some plants, reactor operation without a thermal shield might not be allowed because of pressurized thermal shock (PTS) limitations. Because of the difficulty of inspection, a sensitive, on-line surveillance technique for assuring the integrity of the thermal shield, its supports, and other core internal structures would be valuable.

2. OBJECTIVES

The NRC Core Performance Branch (FIN B0793) and Office of Nuclear Regulatory Research (FIN B0191) have jointly sponsored a feasibility study at ORNL for PWR thermal shield vibration detection using ex-core neutron detector noise. The specific objectives of the study were:

a. Obtain existing neutron noise data from PWRs that have experienced thermal shield degradation and from plants with similar thermal shield designs.

b. Analyze the data and search for systematic changes in the neutron noise which would indicate degradation of the thermal shield or its support structures.

3. SCOPE

The study covered four CE plants: Reactors A, B, C, and D. Noise data from Calvert Cliffs-1 (a CE plant without a thermal shield) obtained through the Neutron Noise Baseline Program (FIN B0191) was also utilized for comparison. Previous studies on thermal shield vibration detection[1] and Sequoyah-1 neutron noise[2] were also utilized. A finite element vibration analysis was performed on a model of a PWR in which degraded thermal shield support conditions were simulated.

4. DESCRIPTION OF PLANTS AND NEUTRON NOISE DATABASE

A short description of each plant is contained in Table 4.1. Figures 4.1-4.5 show the locations of the ex-core neutron detectors. Neutron noise data were obtained in two formats: analog tape recordings and plots of spectral quantities (NPSD, NCPSD, phase, coherence) output from Internals Vibration Monitoring (IVM) systems. Analog recordings were analyzed on ORNL's noise analysis system. Since the plots obtained from IVM systems varied in size and scale from plant to plant and within a plant (see Section on data quality), selected graphical data were digitized on a graphics tablet and replotted on consistent scale sizes for comparison. A description of the data provided by utilities and reactor manufacturers is given in Table 4.2.

5. DATA QUALITY

The ability of noise analysts to interpret noise signatures is directly related to the quality of signal acquisition, conditioning, recording, analysis, and documentation practices. In all cases, ORNL had no control over one or more of these aspects of noise analysis. In the course of our interpretation efforts, deficiencies or discrepancies in the data were noted. Data discrepancies were discounted based on alternate information sources (open literature reports) or our experience with typical neutron noise signature behavior. These discrepancies are listed by reactor type in Table 5.1.

Table 4.1. Description of plants in study

	Reactor A	Reactor B	Reactor C	Reactor D	Calvert Cliffs-1
Power [MW(e)]	810	830	790	478	845
Coolant loops	2	2	3	2	2
Coolant pumps	4	4	3	4	4
Pump speed (rpm)	900	900	1200	1200	900
Thermal shield	Removed*	Removed*	yes†	yes	no

*Thermal shield removed after fuel cycle 5.

†Thermal shield supports repaired after fuel cycle 7.

ORNL-DWG 85-14023

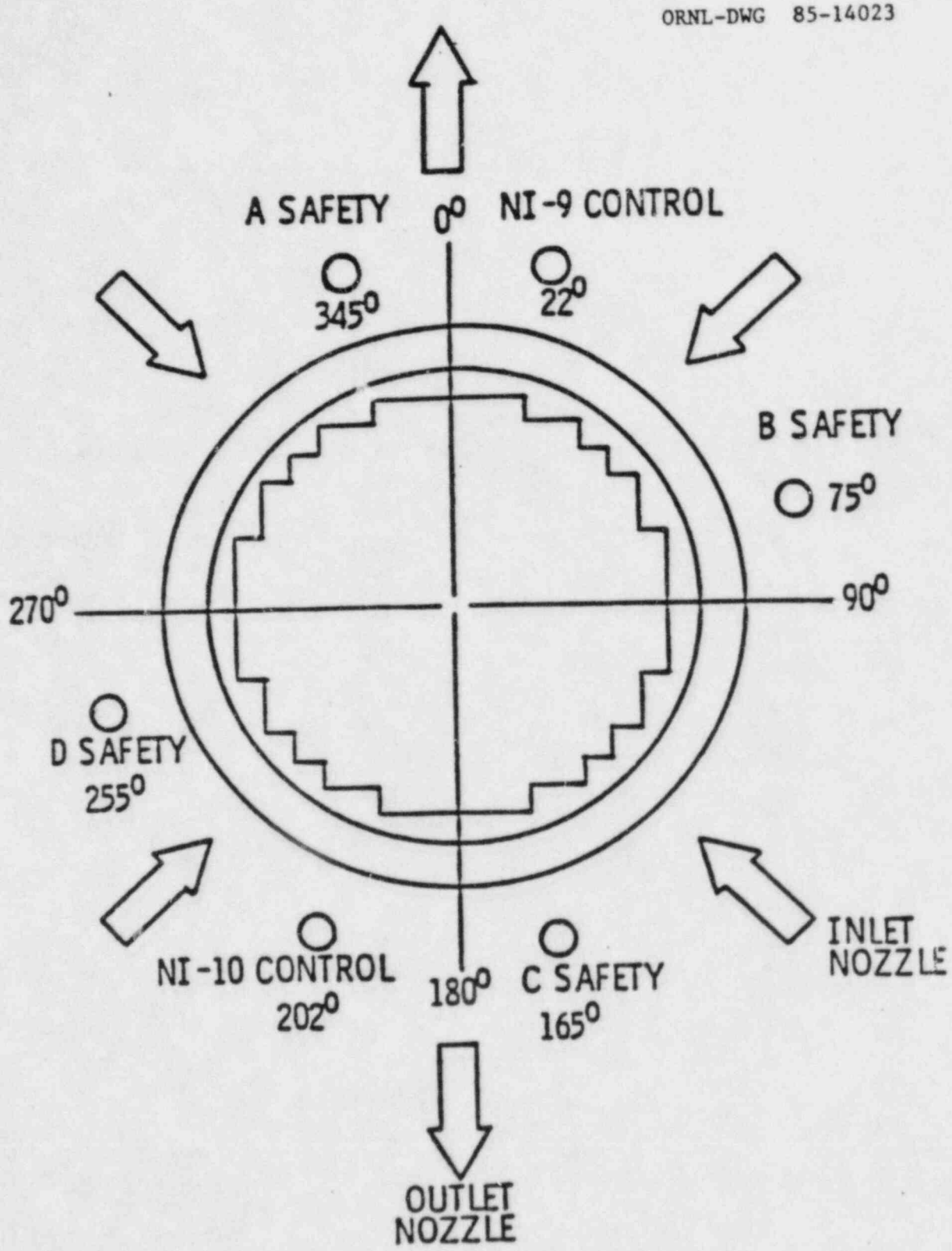

Fig. 4.1. Location of ex-core neutron detectors at Reactor A.

ORNL-DWG 85-14024

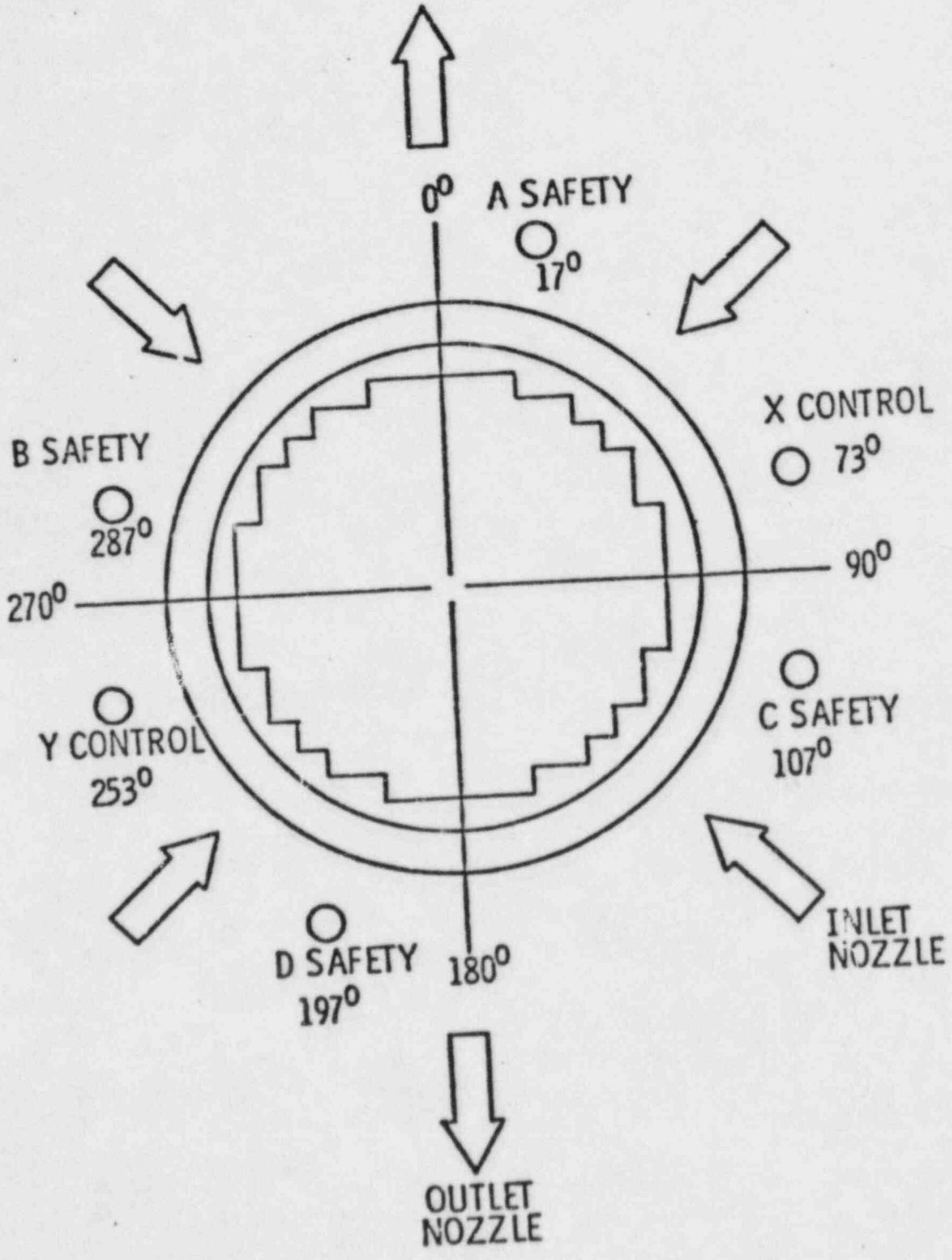

Fig. 4.2. Location of ex-core neutron detectors at Reactor B.

ORNL-DWG 85-14025

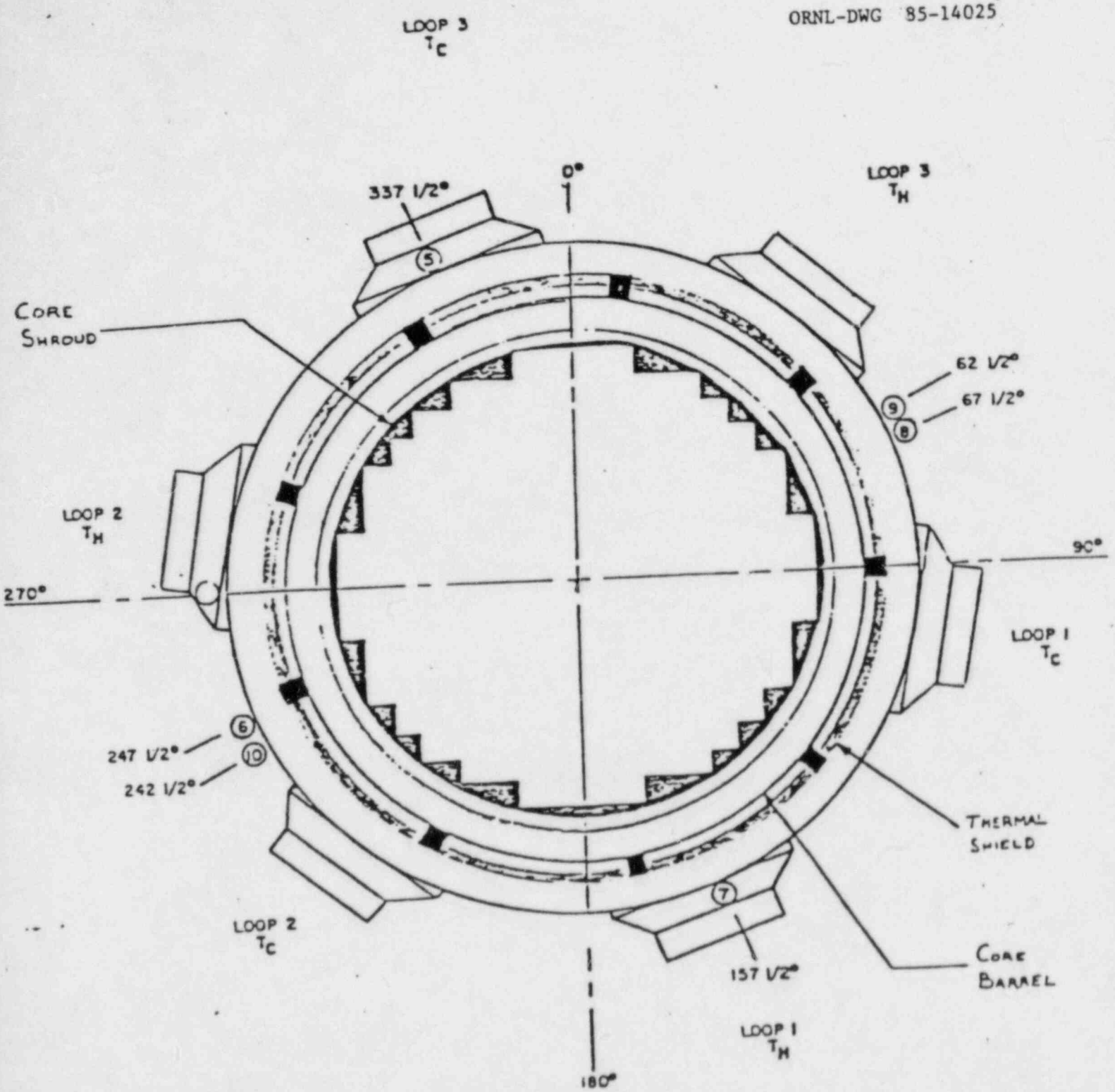

Fig. 4.3. Location of ex-core neutron detectors at Reactor C.

ORNL-DWG 85-14026

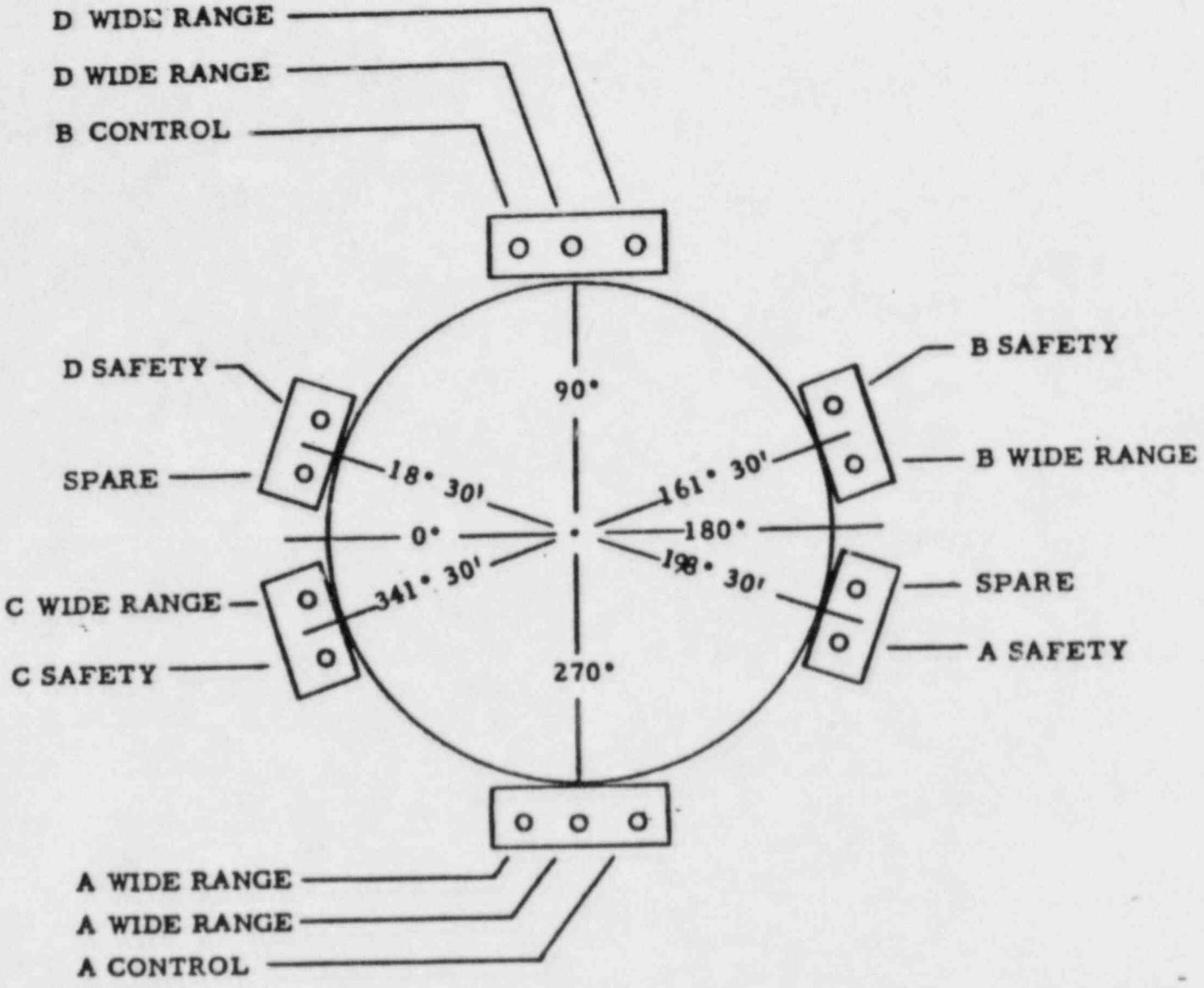

Fig. 4.4. Location of ex-core neutron detectors at Reactor D.

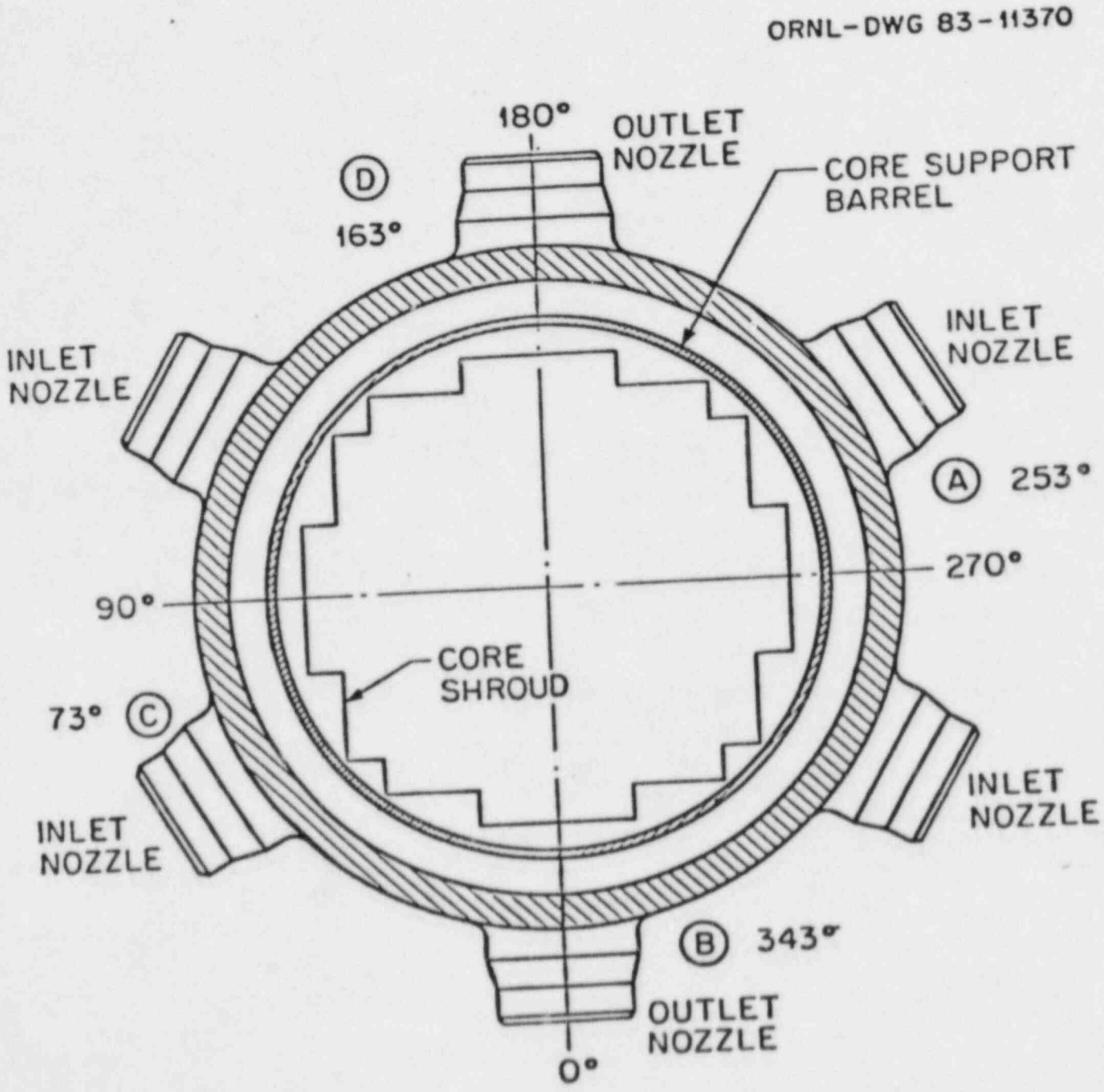

Fig. 4.5 Location of ex-core neutron detectors at Calvert Cliffs-1.

Table 4.2. Data provided to ORNL for thermal shield analysis

	Fuel cycle	Power level (%)	Bandwidth (Hz)
Reactor C			
Tape recordings:	7	100	0.1 - 100
	7	100	0.1 - 200
	7	100	?* - 2K
	7	100	? - 200
	7	100	? - 200
	7	100	? - 200
	8	30	? - 200
	8	48	? - 200
	8	100	? - 200
	8	100	? - 200
Reactor D			
Tape recordings:	3	100	1 - 100
	3	100	1 - 100
	3	100	1 - 100
	3	100	1 - 100
	3	100	1 - 100
	3	100	1 - 100
	3	100	1 - 100
	4	100	1 - 100
	4	100	1 - 100
	4	100	1 - 100
	4	100	1 - 100
	4	100	1 - 100
Reactor A†			
Tape recordings:	5	100	0.1 - 100
IVM plots: (cross core only)	2	100	2 - 12
	2	100	2 - 12
	3	100	2 - 12
	3	100	2 - 12
	4	100	2 - 12
	4	100	2 - 12
	5	100	2 - 12
	5	100	2 - 12
	5	100	0.1 - 15

Table 4.2 (continued)

	Fuel cycle	Power level (%)	Bandwidth (Hz)
Reactor B†			
IVM plots: (cross-core detector only)	1	100	0 - 25
	1	100	0 - 25
	1	100	0 - 25
	1	100	0 - 25
	1	100	0 - 25
	1	100	0 - 25
	1	100	0 - 25
	1	100	0 - 25
	1	100	0 - 25
	1	100	0 - 25
	1	100	0 - 25
	1	100	0 - 25
	1	100	0 - 25
	1	100	0 - 25
	1	100	0 - 25
	1	100	0 - 25
	1	100	0 - 25
	1	100	0 - 25
	1	100	0 - 25
	1	100	0 - 25
	1	100	0 - 25
	1	100	0 - 25
	2	50	0 - 25
	2	100	0 - 25
	2	100	0 - 25
	2	100	0 - 25
	2	100	0 - 25
	2	100	0 - 25
	2	100	0 - 25
	2	100	0 - 25
	2	100	0 - 25
	2	100	0 - 25
	2	100	0 - 25
	2	100	0 - 25
	2	100	0 - 25
	2	100	0 - 25
	2	100	0 - 25
	2	100	0 - 25
	2	100	0 - 25
	2	99	0 - 25
	3	50	0 - 25
	3	100	0 - 25

Table 4.2 (continued)

Fuel cycle	Power level (%)	Bandwidth (Hz)
3	100	0 - 25
3	100	0 - 25
3	100	0 - 25
3	100	0 - 25
3	100	0 - 25
3	100	0 - 25
3	100	0 - 25
3	100	0 - 25
3	100	0 - 25
3	100	0 - 25
3	100	0 - 25
3	100	0 - 25
3	100	0 - 25
3	100	0 - 25
4	50	0 - 25
4	100	0 - 25
4	100	0 - 25
4	100	0 - 25
4	100	0 - 25
4	100	0 - 25
4	100	0 - 25
4	100	0 - 25
4	100	0 - 25
4	100	0 - 25
4	100	0 - 25
4	100	0 - 25
4	100	0 - 25
4	100	0 - 25
4	100	0 - 25
5	100	0 - 25
5	100	0 - 25
5	100	0 - 25
5	100	0 - 25
5	100	0 - 25
5	100	0 - 25
5	100	0 - 25
5	100	0 - 25
5	100	0 - 25
5	100	0 - 25
5	100	0 - 50
5	96	0 - 50

Table 4.2 (continued)

Fuel cycle	Power level (%)	Bandwidth (Hz)
6	83	0 - 25
6	100	0 - 50
6	100	0 - 50
6	100	0 - 25
6	100	0 - 50
6	100	0 - 50
6	100	0 - 50
6	100	0 - 50

*? indicates value unknown.
†IVM data analysis bandwidth only. Amplifier and filter settings unknown.

Table 5.1. Data discrepancies and deficiencies

Reactor	Data format	Discrepancy or deficiency
Reactor A	Tape	Detectors Safety A or Safety C mislabeled
	IVM	Cross-core detectors only
Reactor B	IVM	Drawing of ex-core detector locations incorrect. Inconsistent plot scales. Mislabeled plot units. Probable incorrect data normalization. Possible low signal dynamic range. Amplifier bandwidth unknown. Cross core detectors only.
Reactor C	Tape	High pass filter setting not recorded on some runs. Isolation amplifiers gain discrepancy on some runs.
Reactor D	Tape	Likely tape recorder speed variation during recording or copying process.

Data quality is also determined by the statistical uncertainty in analysis results. The IVM data provided by utilities and reactor manufacturers were typically analyzed using only 50 ensemble averages. The resulting statistical uncertainty in a single frequency estimate of a power spectral density (PSD) is approximately 14% of the value at the 1 standard deviation confidence level. Statistical confidence in cross-spectral quantities (phase and cross power spectral densities) are not known at present since uncertainty in these values are dependent upon both the number of ensemble averages and the coherence between the signals. For 50 ensemble averages, coherences must exceed 0.06[3] to be considered statistically significant.

Statistical confidence and frequency resolution also determine the uncertainty of resonant frequencies in the spectra. In general, broader resonances with higher statistical uncertainty in their amplitude and frequency resolution will lead to lower confidence in determining the actual center frequency of the resonance.

6. MODELS OF THERMAL SHIELD VIBRATION AND NEUTRON NOISE

6.1 FINITE ELEMENT VIBRATION MODEL

6.1.1 Description of Models

Five finite element models of the reactor core and core support structures for a typical PWR were studied.* Each of these models includes a half-symmetric representation of the core and core support structure system as shown in Fig. 6.1. The model shown in Fig. 6.1 represents the baseline case and includes the core barrel, core support shield, thermal shield, plenum and lower grid, a simulated fuel assembly representation, and a full complement of attachments between the core barrel and thermal shield.

The other four models represent variations on this baseline case, and are designed to simulate various forms of thermal shield support degradation: upper radial attachment missing over a 60° sector, no upper radial attachment, degraded lower attachment with no upper attachment, and no thermal shield. A schematic representation of these cases is presented in Fig. 6.2.

The PAFEC (Program for Automatic Finite Element Calculations) computer program was used to perform the analysis for this study. PAFEC is a general-purpose, three-dimensional linear and non-linear finite element analysis program.* The PAFEC program was used to determine natural frequencies and normal mode shapes of the core internal structures in water for the five models presented.

---

*The analysis was performed on a B&W type plant because of availability of structural details. While the thermal shield supports assumed are different from those of a CE plant, we would expect the same predicted trends. Verification of this assumption is beyond the scope of this study.

ORNL-DWG 85-14027

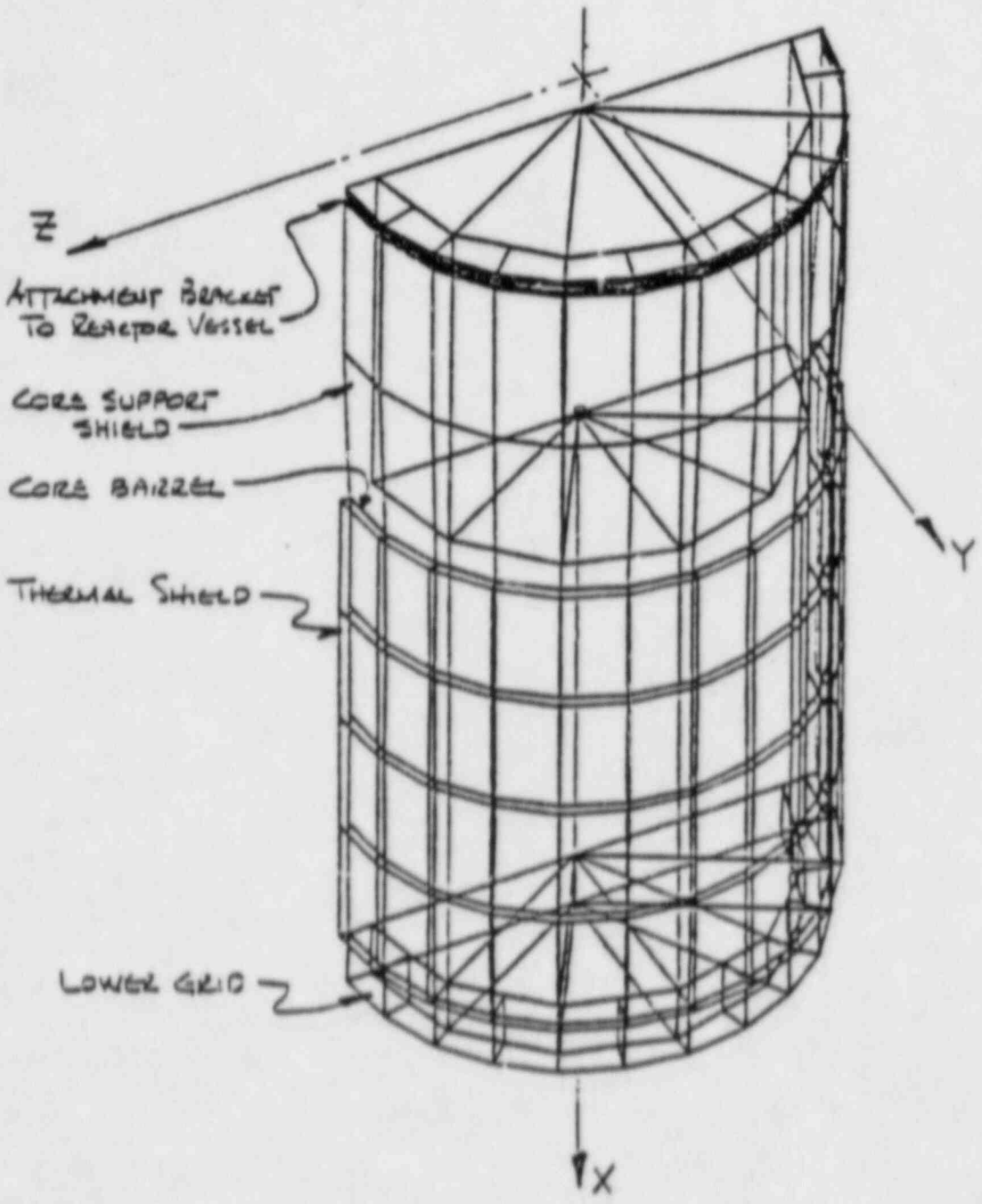

Fig. 6.1. Finite element model of baseline (undegraded) system with thermal shield.

ORNL-DWG 85-14028

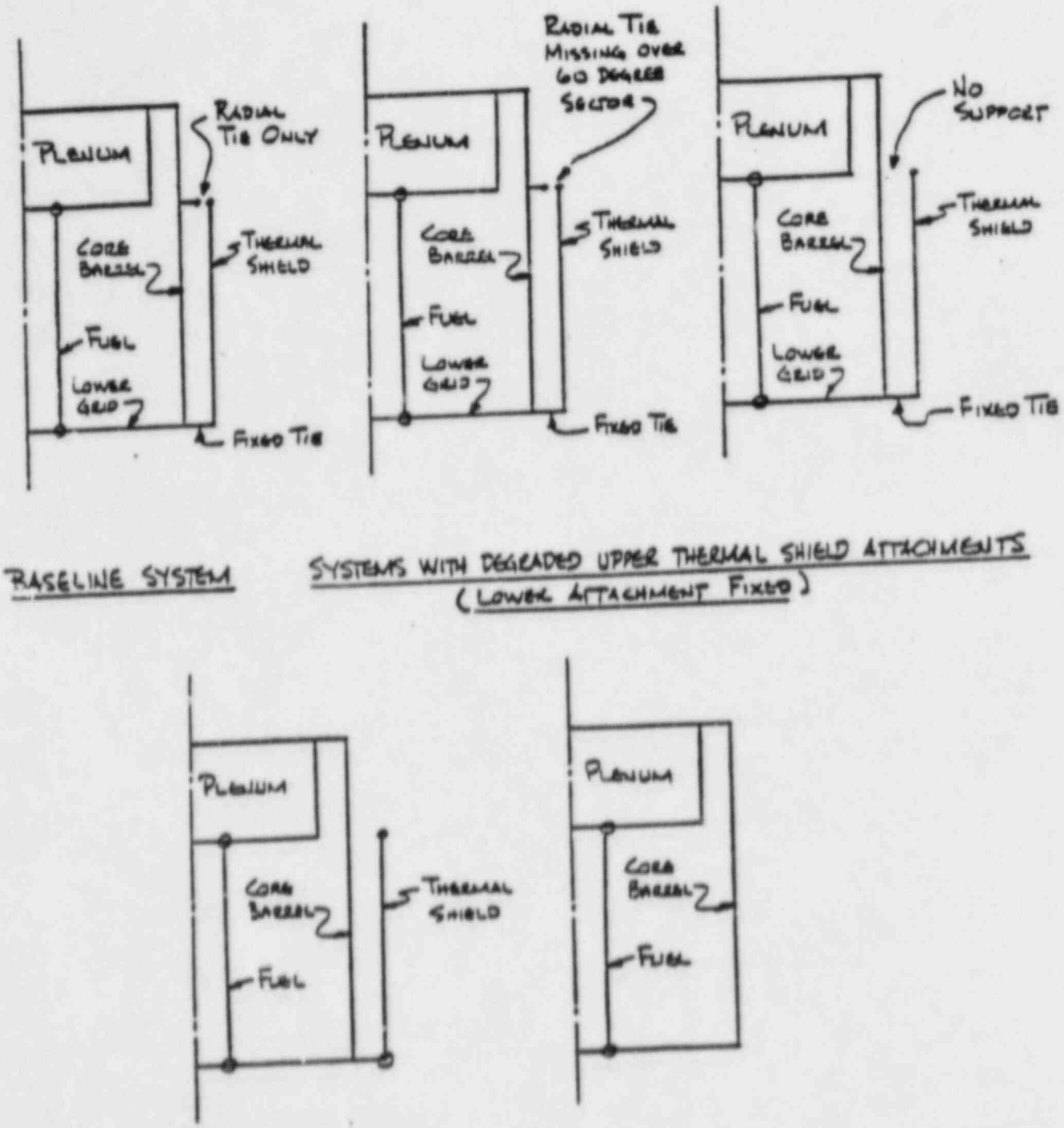

Fig. 6.2. Schematic representation of finite element models of degraded thermal shield supports.

6.1.2 Results of Vibration Model

Table 6.1 presents a summary of the natural frequencies and mode shapes of the core barrel and thermal shield.* The fuel assembly bending mode frequency was fixed in the model at 3.47 Hz. The results predict the following behavior of core internals vibrations:

1. In the baseline (undegraded) case, the core barrel and thermal shield do not act independently (i.e., they vibrate as a unit).
2. As thermal shield support degradation occurs, we postulate that two processes lead to changes in the core barrel/thermal shield beam mode frequency: changes in stiffness and changes in effective mass (the true mass and the added mass resulting from resistance of motion of a structure in water) of the combined system. Each process leads to changes in the beam mode resonant frequency in opposite directions. As the thermal shield becomes decoupled from the core barrel due to upper attachment degradation, the core barrel/thermal shield system becomes less stiff, and the resonant frequency of the system decreases. When both upper and lower attachments are degraded, the thermal shield is increasingly decoupled from the system, reducing its effective mass. The reduction in effective mass leads to an increase in the beam mode resonant frequency.
3. When both the upper and lower attachments are degraded, independent thermal shield shell mode vibrations appear. These vibrations occur at a lower frequency than the combined core barrel/thermal shield system shell mode.

---

*No attempt was made to adjust the model parameters (other than the fuel assembly bending mode frequency) to produce frequencies matching neutron noise results. The intent of these studies was to determine, qualitatively, changes in core internals vibration frequencies resulting from thermal shield support degradation.

Table 6.1. Summary of calculated natural frequencies and mode shapes for finite element models of degraded thermal shield supports in a B&W reactor

Mode of vibration	Baseline (Hz)	60° Degraded upper attachments (Hz)	No upper attachments (Hz)	No upper attachments, Degraded lower attachments (Hz)	No thermal shield (Hz)
Fuel assembly bending*	3.47	3.47	3.47	3.47	3.47
Core barrel and thermal shield beam mode	15.17	15.12	15.03	16.28	16.30
Core barrel and thermal shield (3 node)	31.2	31.05	36.43	33.54	34.25
Thermal shield shell modes:					
1 node (oval)				3.66	
2 node			22.67	10.88	
3 node			24.00	22.03	

*This frequency was held constant for all cases considered.

4. Changes in the core/barrel/thermal shield beam mode frequency are small (<1.5 Hz) even for severely degraded thermal shield attachments (including the case in which the thermal shield was removed entirely).

It was also observed that vibrational amplitudes and mode shapes are axially dependent upon how the thermal shield is supported and where the support degradation occurs.

6.2 NEUTRONIC MODELS

Neutronic models have been developed to infer amplitudes of thermal shield or CSB vibrations from ex-core neutron noise. We reviewed* these models with the following results:

1. Thermal shield and CSB scale factor* calculations assume that fuel vibrations do not contribute to the ex-core neutron noise. Experimental results do not support this assumption.
2. Thermal shield scale factor calculations assume that the structure vibrates independently of the CSB. Experimental and calculational results (see Sect. 6.1) do not support this assumption.
3. Scale factor calculations indicate that independent vibrations of the thermal shield produce 500% less ex-core neutron noise than CSB motion for a given amplitude of vibration.

We conclude from these results that commonly utilized neutronic models and calculational techniques are inadequate for determining the amplitude of internals vibrations. Because of the difficulty in interpreting amplitude changes in the neutron noise we recommend* that

---

*The "scale factor" is a number, usually obtained through shielding-type calculations, which converts neutron noise amplitude to vibrational amplitude of a core internal structure (i.e., percentage of neutron noise per mil of vibration).

surveillance of core internals be performed by observing long-term changes in the neutron noise, combined with accelerometer measurements. Such accelerometer measurements may require optimal sensor location, mounting, and signal conditioning (which is likely beyond the capabilities of many loose parts monitoring systems). Other workers[6] have also reached the same conclusions and have therefore installed vibration sensors on the pressure vessel upper head to supplement neutron noise measurements.

7. DATA OBSERVATIONS

7.1 REACTOR A

At the beginning of fuel cycle 2 (BOC2), normalized power spectral densities (NPSDs) and normalized cross-power spectral densities (NCPSDs) of cross-core detectors Safety A and Safety C exhibit* three broad resonances at 3.1, 6.5, and 14.1 Hz as shown in Fig. 7.1. Coherences between cross-core detectors are high (approximately 0.8) over the 3- to 8-Hz region as shown in Fig. 7.2 and have a 180° phase relationship, which is typical of pendular (beam-mode) structural vibrations. The 14.1-Hz resonance also exhibits high cross-core detector coherence (0.6-0.8) but the phase is ~0°, which is typical of shell-mode type vibrations. The cross-core coherence also displays a resonance at approximately 20 Hz, which is not clearly evident in the NCPSDs† and which has ~0° phases typical of shell mode vibrations.

At the BOC5 (the last fuel cycle before thermal shield damage was discovered), the 3.1- and 6.5-Hz resonances had both become sharper and had shifted to 1.5 and 7.5 Hz respectively, as shown in Fig. 7.1. Phases remained at 180° while coherences were no longer uniformly high over the 3- to 8-Hz range. In this range, isolated resonances became visible in the coherence at 1.5, 4, and 7.6 Hz as shown in Fig. 7.2. The evolution of changes in the frequency of the 3-Hz resonance is displayed in Fig. 7.3 versus the fuel cycle. Until EOC3, this resonance

---

*IVM data from Reactor A is bandpassed in the 2- to 14-Hz range. Some information in the spectra may be present at frequencies outside this range (since the analysis range was 0.3-25 Hz). This information, however, will be heavily influenced by the signal conditioning filter characteristics. These observations are true for the analog tape data which was conditioned and analyzed over the 0.1- to 40-Hz range.

†The resonance is more clearly visible in the tape data. The resonance may be difficult to resolve in the IVM data due to the filter roll-off.

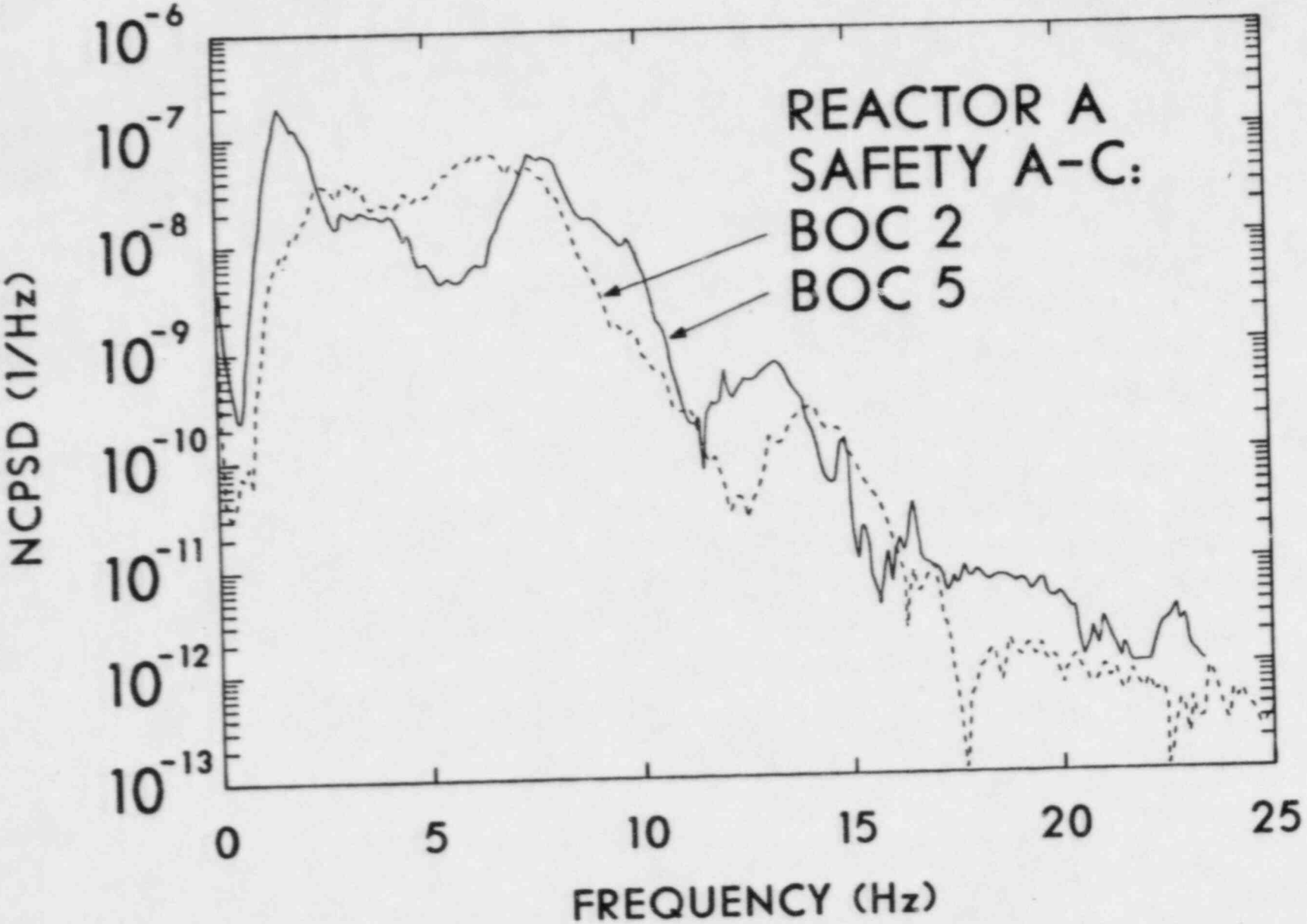

Fig. 7.1. Normalized cross-power spectral densities (NCPSDs) of cross-core detector pair Safety A and Safety C at Reactor A for beginning of fuel cycles (BOC) 2 and 5 (before thermal shield removal).

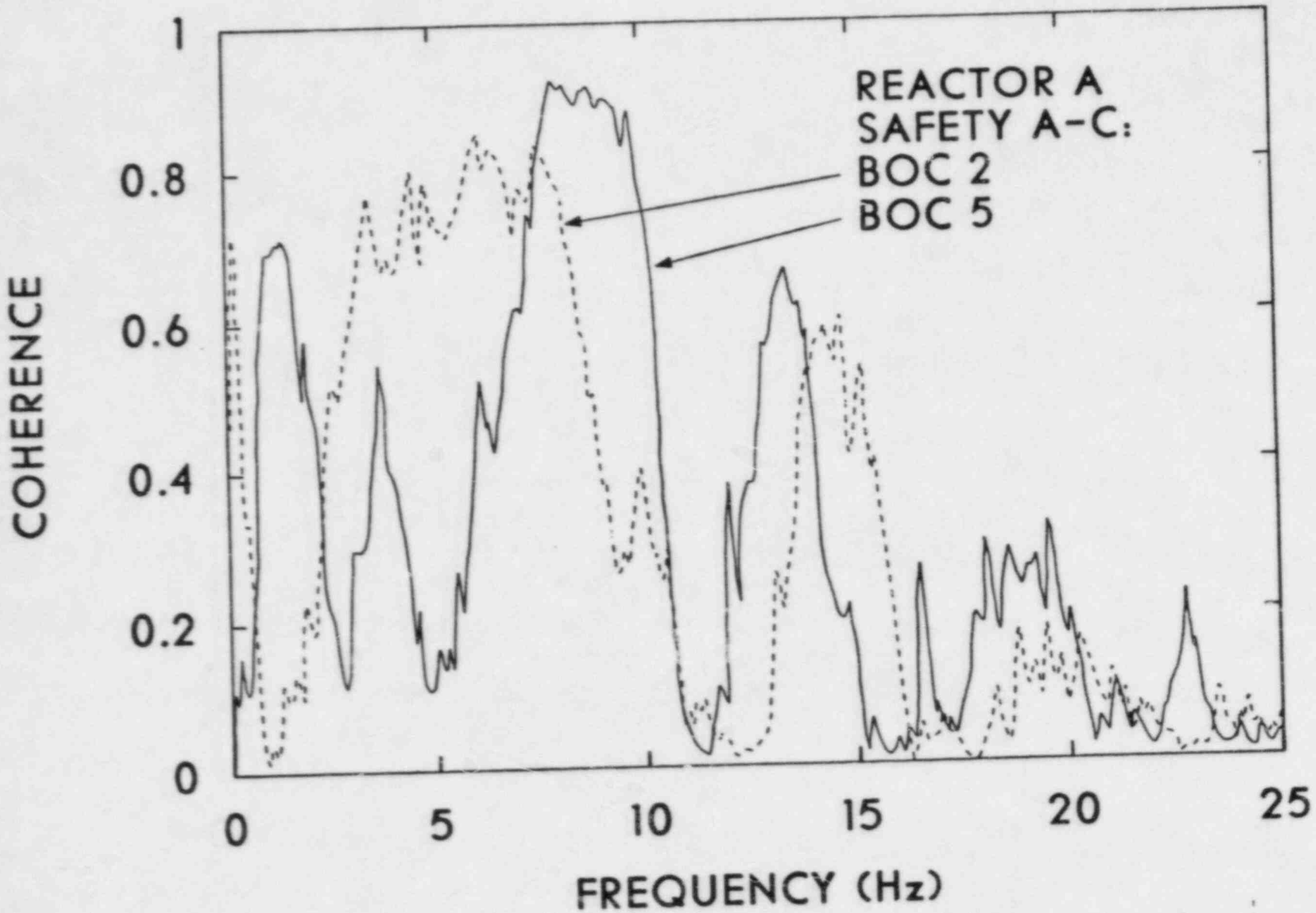

Fig. 7.2. Coherences for cross-core detector pair Safety A and Safety C at Reactor A for BOC 2 and BOC 5.

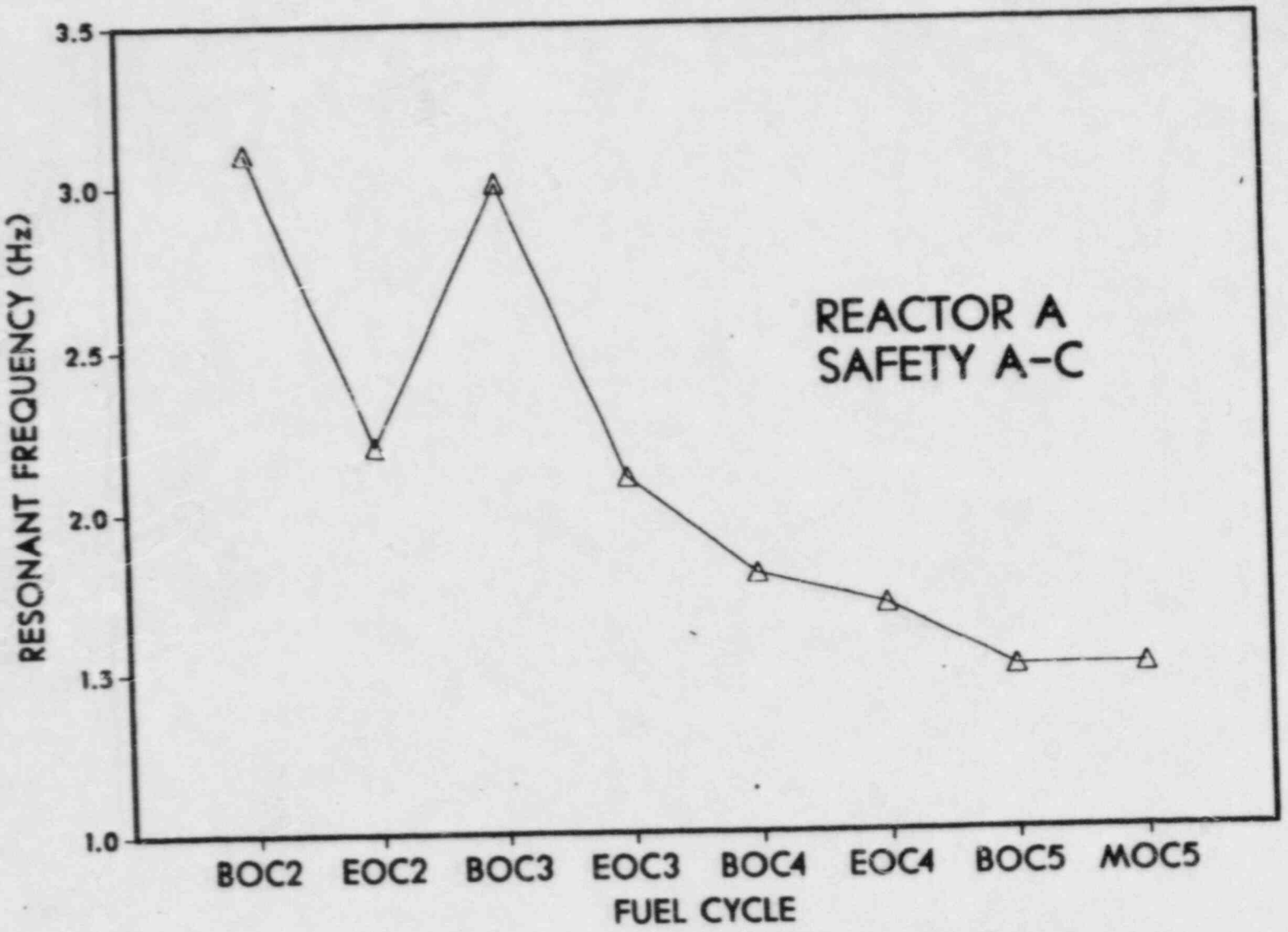

Fig. 7.3. Frequency evolution of the 3-Hz resonance in the NCPSD of cross-core detector pair Safety A and Safety C at Reactor A.

behaved in a manner similar to that experienced in other PWRs: decrease in frequency over the fuel cycle due to fuel assembly grid spacer relaxation and increase in frequency at the beginning of the next cycle due to new fuel being loaded. After EOC3, however, the resonance continued to decrease in frequency to 1.5 Hz. This frequency is lower than that normally experienced in other PWRs.

The 6.5-Hz resonance, which is normally associated with beam mode core barrel motion and the second mode of fuel assembly vibration, was observed to increase in frequency over the first three fuel cycles (Fig. 7.4). The largest frequency changes (6.5 to 7.7 Hz) occurred over cycles 2 and 3. This increase in frequency is significant since it is in the opposite direction expected for fuel assembly resonant frequency changes. Changes in frequency of this resonance between the end and beginning of a fuel cycle are indicative of either changes in fuel assembly vibrations excited by CSB motion (as has been observed in other PWRs) or changes in the CSB/thermal shield structural dynamics during refueling (as might be caused by thermal cycling or changes in CSB hold-down forces).

The 14.1-Hz resonance (Fig. 7.5) also showed a decrease in frequency (14.1 to 13.3 Hz), occurring primarily during the second and third fuel cycles. Unlike the 3- and 6.5-Hz resonances there was no frequency change between fuel cycles. Cross-core detector phases were 0° for all measurements.

7.2 REACTOR B

Because the data provided ORNL were plotted on non-uniform scales (see Sect. 5), it is not possible to show evolution of NPSDs or NCPSDs. Coherences and phases were, however, usable since gains and normalizations generally do not affect these quantities. Cross-core detector coherence at BOC1 displayed high (0.8) coherence over the 3- to 8 region, as shown in Fig. 7.6 and had a 180° phase relationship. At the

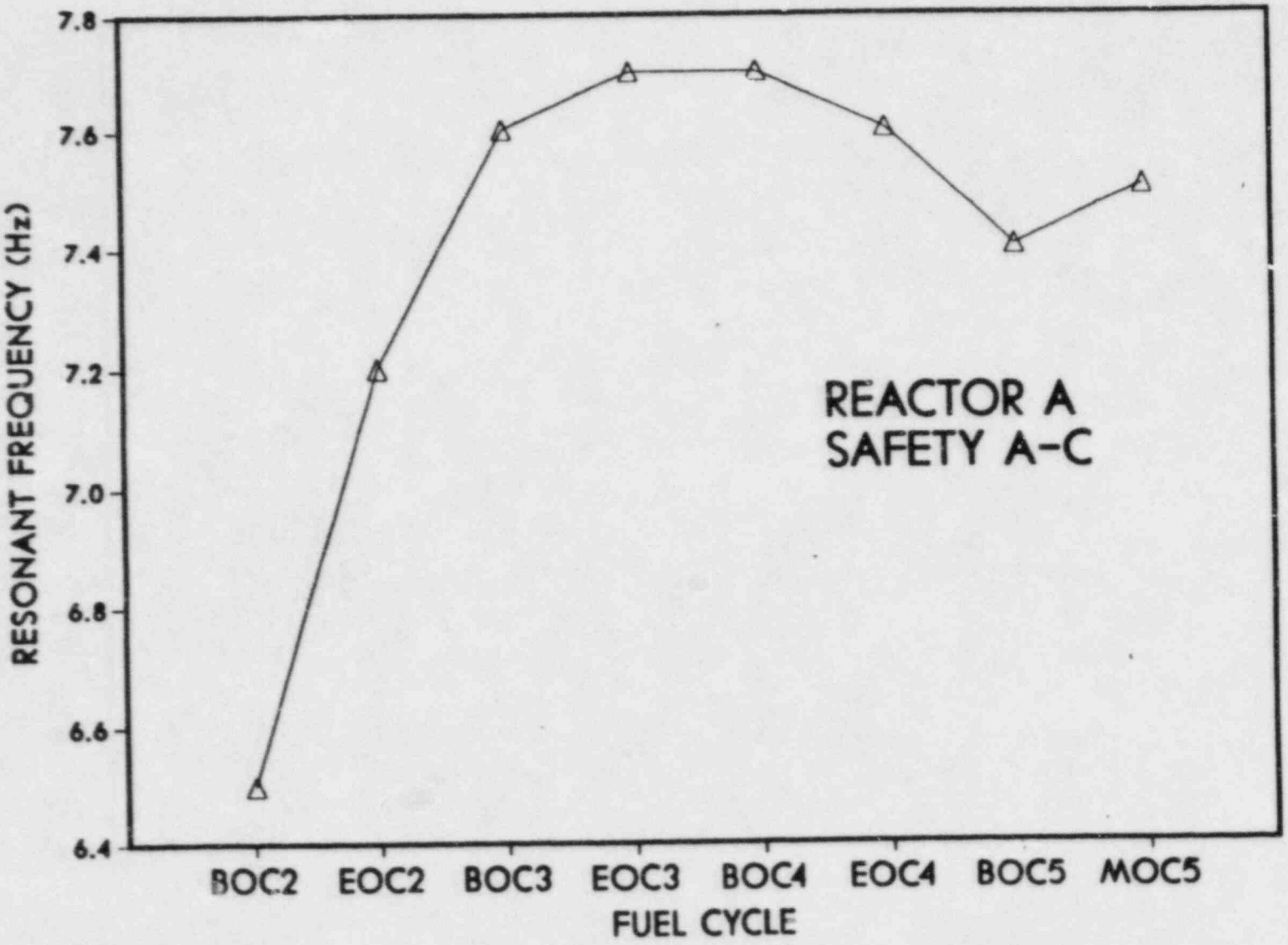

Fig. 7.4. Frequency evolution of the 6.5-Hz resonance in the NCPSD of cross-core detector pair Safety A and Safety C at Reactor C.

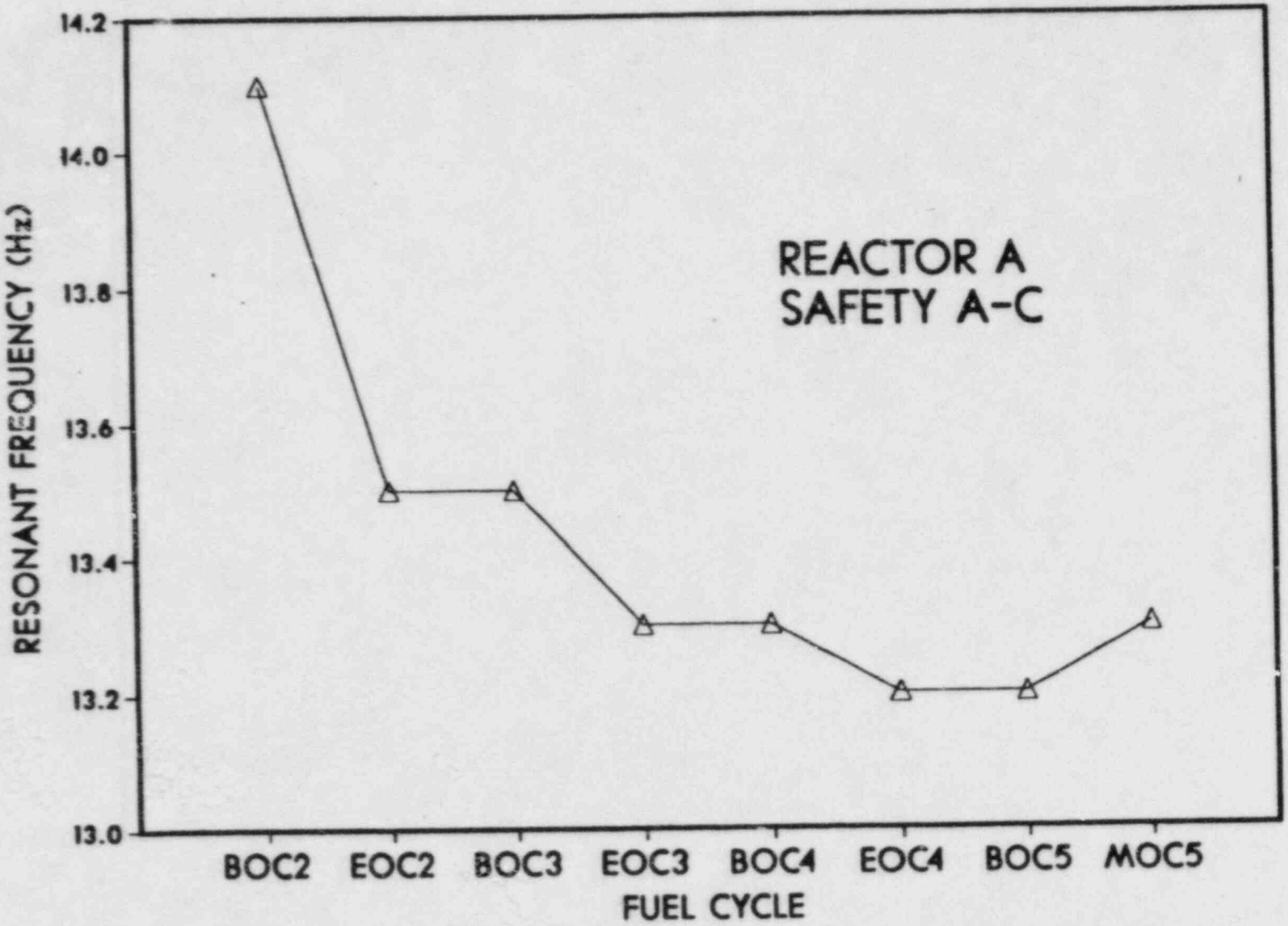

Fig. 7.5. Frequency evolution of the 14.1-Hz resonance in the NCPSD of cross-core detector pair Safety A and Safety C at Reactor A.

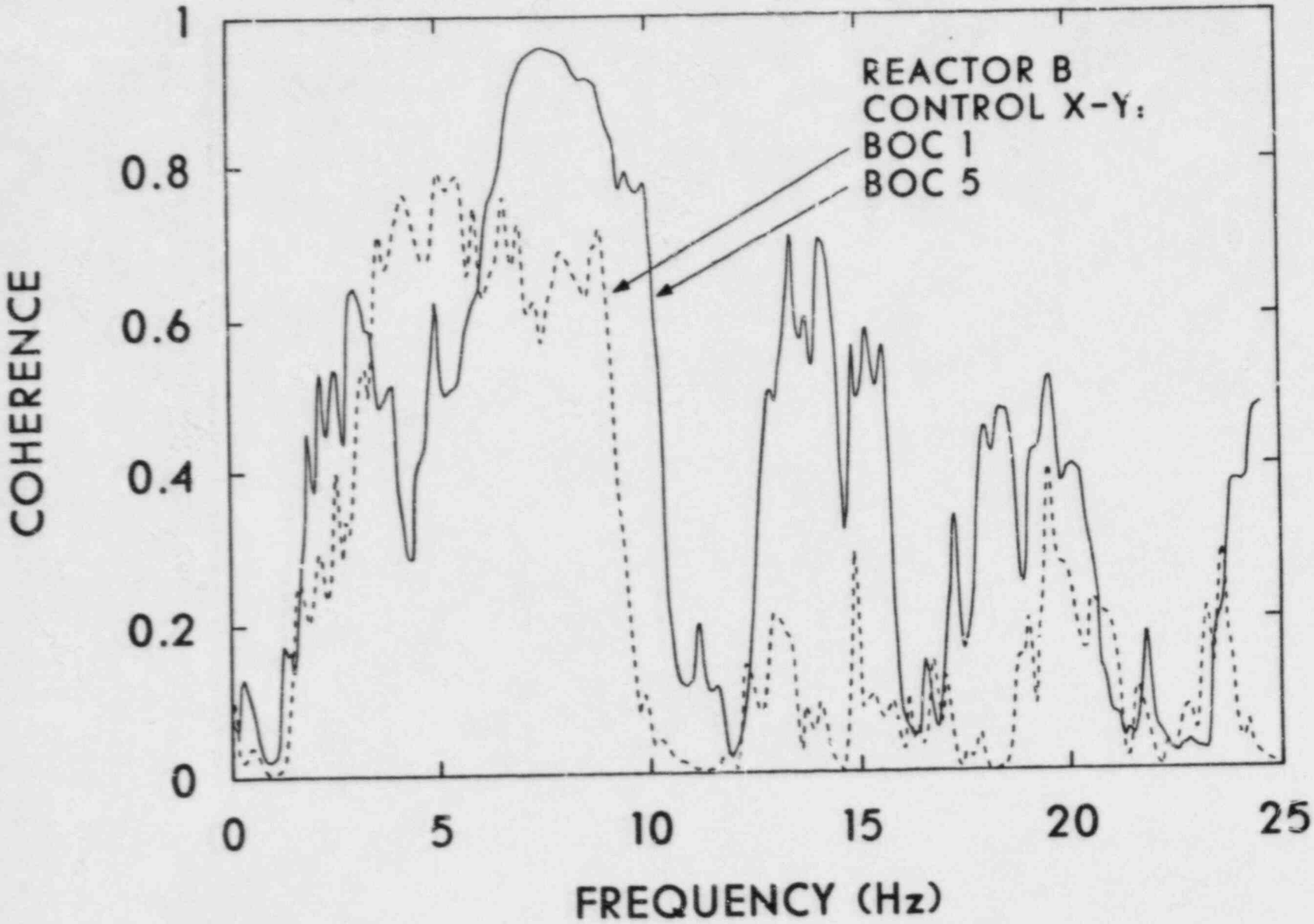

Fig. 7.6. Coherences between cross-core detector pair Control X and Control Y at Reactor B for BOC 1 and BOC 5.

BOC1, resonances were barely visible at 14.1 or 20 Hz in the NPSDs or NCPSDs, and coherences at these frequencies were <0.4.

At the BOC5 (last fuel cycle before thermal shield support degradation was discovered), the coherence in the 14-Hz region had increased to 0.7 and to 0.5 in the 20-Hz region, as shown in Fig. 7.6. The coherences in the 7-Hz region increased to nearly 1 and a distinct resonance could be resolved in the coherence at 3 Hz. The resonances in these frequency ranges were always broad so that it is difficult to determine their exact frequency. In general, the 14-Hz resonance decreased to -13 Hz and the 6.3-Hz resonance increased to -7.0 Hz as shown in Figs. 7.7 and 7.8 respectively. Phases in the 7.0-Hz range for cross-core detectors were always 180° and 0° in the 14-Hz and 20-Hz regions, respectively.

After cycle 5, damage to the thermal shield supports was discovered. During the outage following cycle 5, the thermal shield and its supports were removed. During fuel cycle 6, the reactor was operated without a thermal shield. Significant differences can be seen in the cross-core detector coherences, particularly in the 10- to 25-Hz range, as shown in Fig. 7.9. During fuel cycles 5 and 6, signal conditioning and analysis were expanded to include the 25- to 50-Hz frequency range. These results, presented in Fig. 7.10, show that significant changes occurred in the cross-core detector coherences above 25 Hz (note that the high coherence appearing at 40 Hz is most likely due to 60-Hz electrical noise aliased by the 100-Hz sampling rate employed in the analysis).

7.3 REACTOR C

During a refueling outage at the EOC6, two upper thermal shield positioning pins were found to be dislodged, and a third pin was found loose. These pins, along with others, were either replaced or tightened at the EOC7 refueling outage. We received neutron noise tape recordings made on 6 occasions previous to the refueling outage and on 5 occasions following repairs.

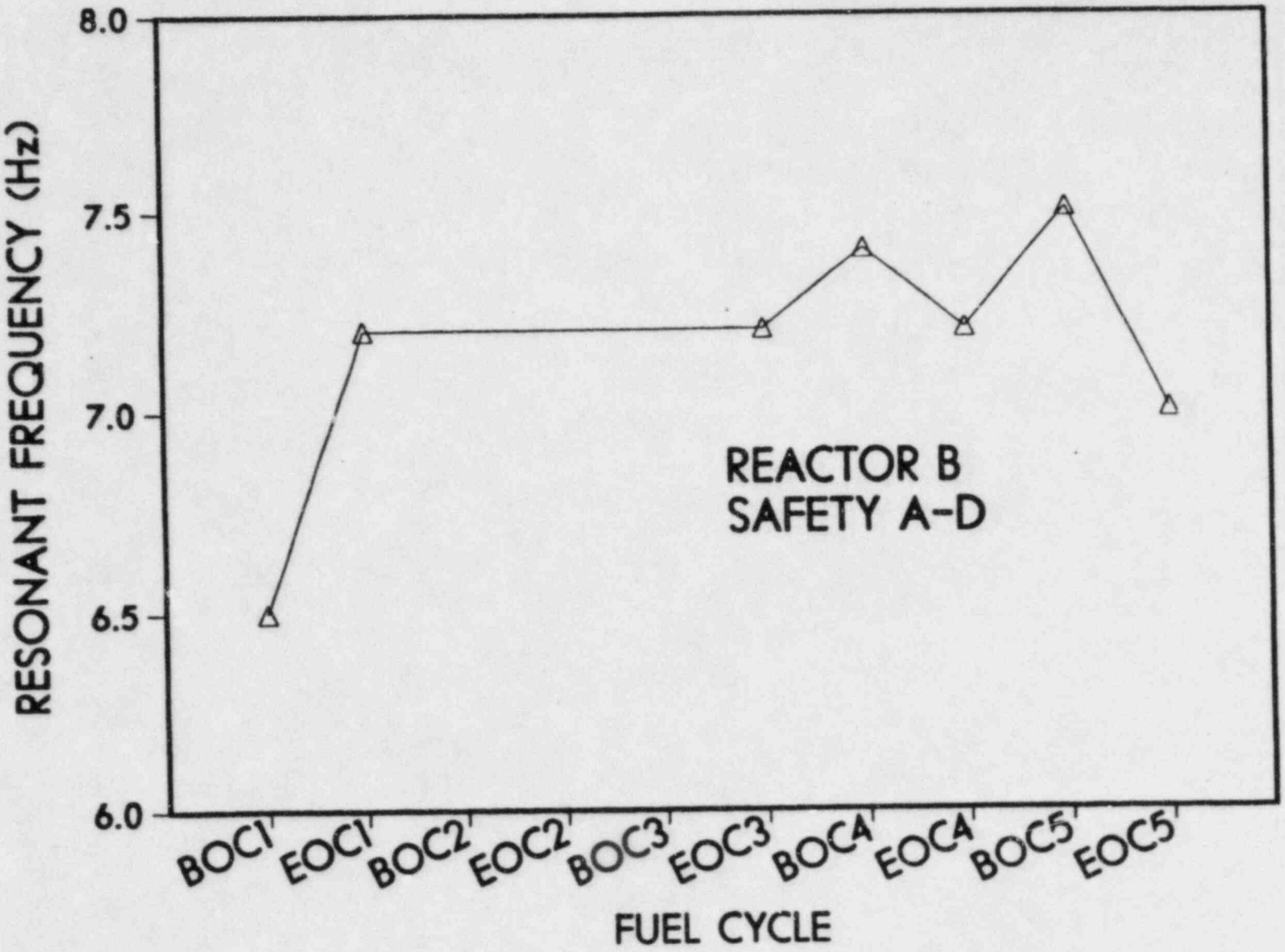

Fig. 7.7. Frequency evolution in the 6.5-Hz resonance in the NCPSD of cross-core detector pair Safety A and Safety D at Reactor B.

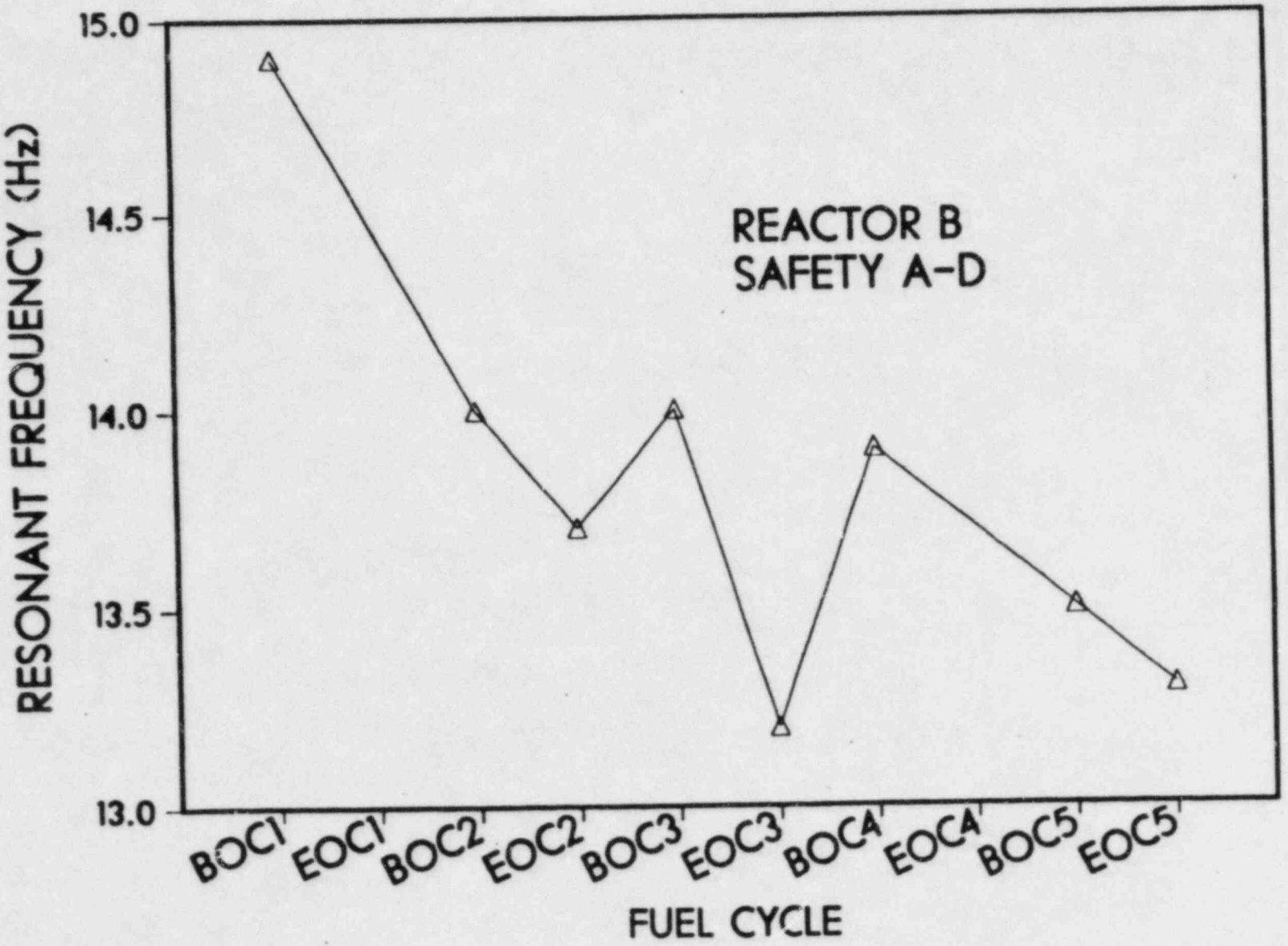

Fig. 7.8. Frequency evolution in the 14-Hz resonance in the NCPSD of cross-core detector pair Safety A and Safety D at Reactor B.

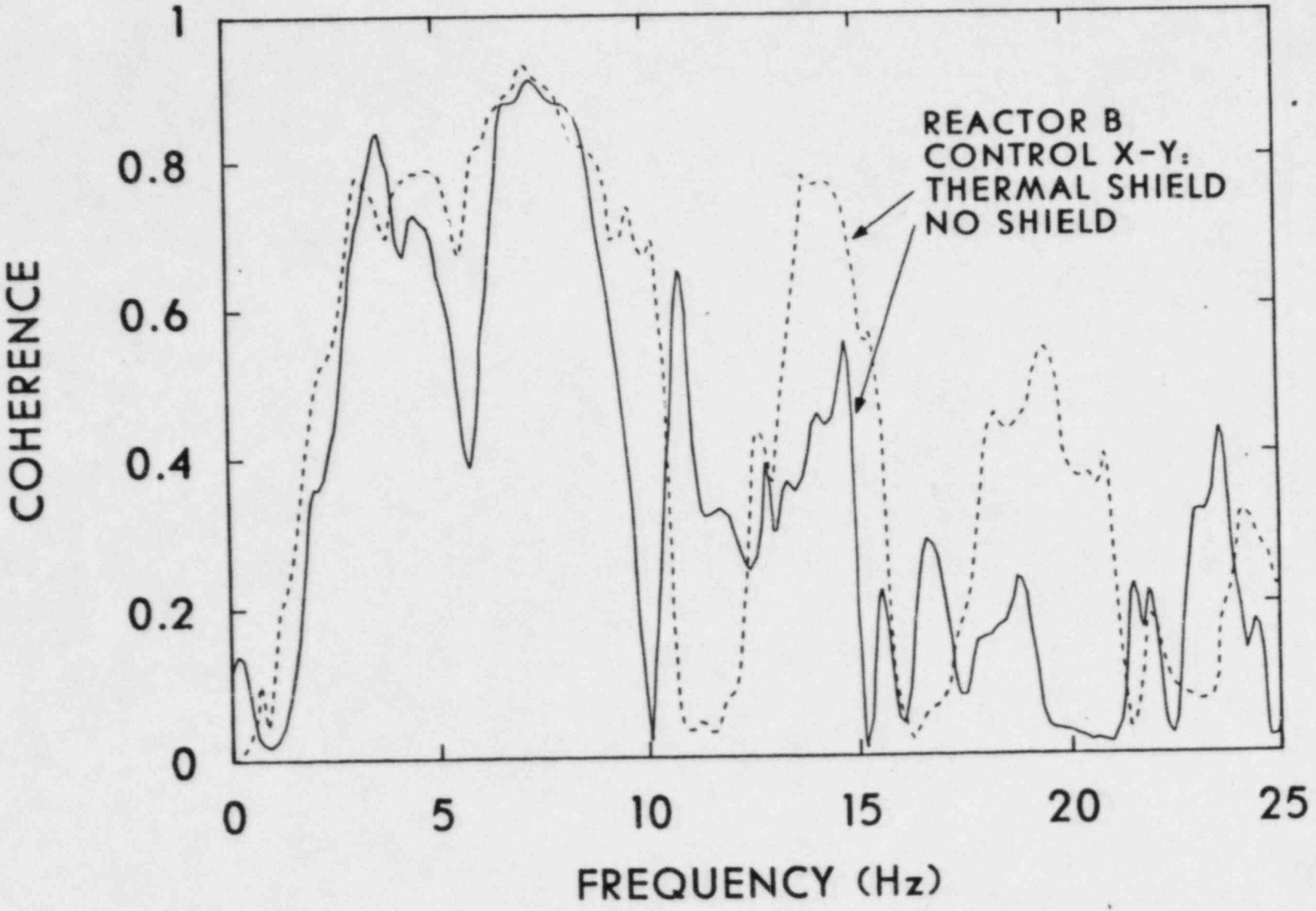

Fig. 7.9. Coherence between cross-core detector pair Control X and Control Y below 25 Hz at Reactor B for operation with thermal shield (EOC5) and without thermal shield (EOC6).

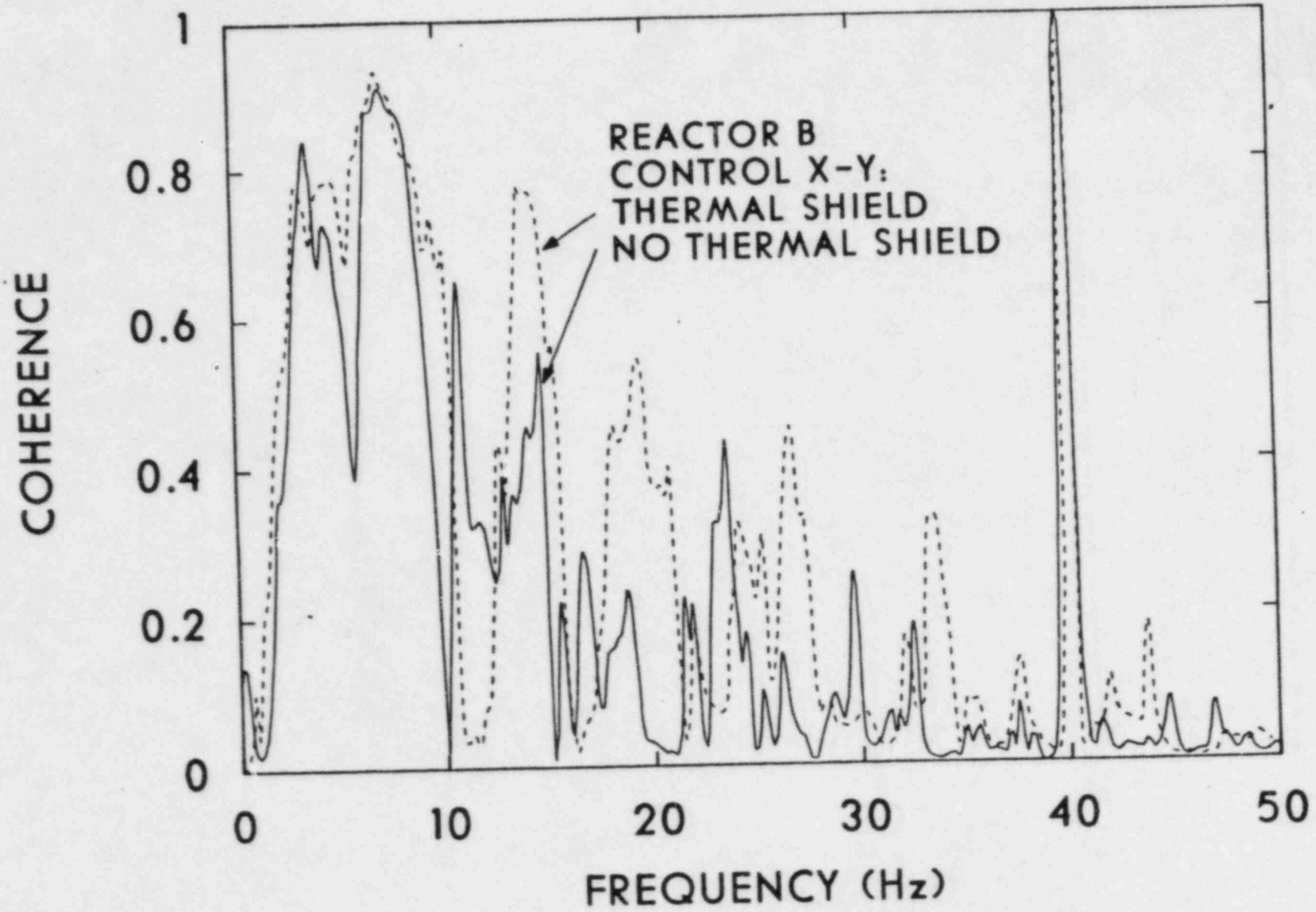

Fig. 7.10. Coherences between cross-core detector pair Control X and Control Y at Reactor B below 50 Hz for operation with thermal shield (EOC5) and without thermal shield (EOC6).

Figure 7.11 shows a comparison between cross-core detector NCPSDs taken at MOC7 and EOC7 (immediately prior to the refueling outage). Only slight differences in NCPSD and NPSD magnitudes were observed between these two measurements, but no differences were observed in the phases or coherences. A comparison between pre- and post-repair (MOC7 and BOC8 respectively) measurements shows some differences in NCPSD magnitudes in the 3- to 9-Hz, 9- to 12-Hz, and 30- to 35-Hz frequency ranges as shown in Fig. 7.12.

The normalized root-mean squared (NRMS) values over the 3- to 9- and 9- to 12-Hz frequency ranges are plotted against time and shown in Figs. 7.13 and 7.14 respectively. These plots show a large decrease in the NRMS after repairs to the thermal shield supports were performed during the EOC7 outage. When these data are plotted against soluble boron concentration, however, the NRMS are shown to decrease monotonically with increasing soluble boron concentration as shown in Figs. 7.15 and 7.16. No changes in phase or coherence were observed before and after repair of the thermal shield.

7.4 REACTOR D

In Fig. 7.17, cross-core detector NCPSDs from tape recordings made on BOC4 and MOC4 are compared. Below 25 Hz, changes can be observed in both the amplitudes and the frequencies of resonances. The resonance centered at about 7.5 Hz displays a beam-mode type behavior, while a large resonance at ~17 Hz shows an in-phase behavior. These resonances, including a low-amplitude sharp resonance at 20 Hz (which corresponds to the pump rotation speed of 1200 rpm), show decreases in frequency of ~0.5 Hz during cycle 4. Because pump speeds are usually constant, we suspected that the observed frequency shifts were more likely the result of speed degradation in the tape recording or copying operations. To confirm this hypothesis, we analyzed 60-Hz contamination on the tape recordings. The 60-Hz noise was found to decrease to 59.5 Hz, thus confirming our hypothesis.

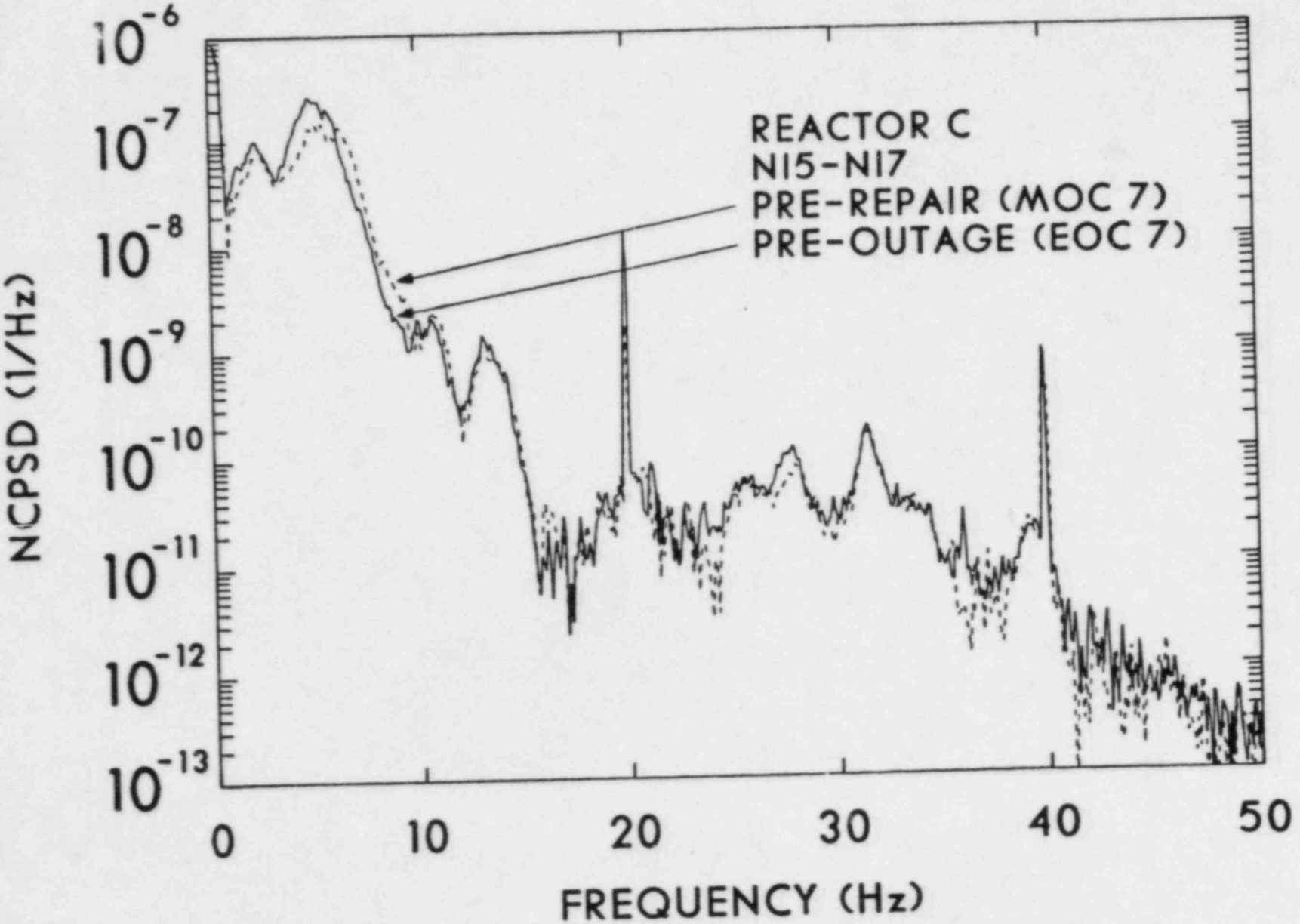

Fig. 7.11. Comparison between NCPSDs for cross-core detector pair NI 5 and NI 7 at Reactor C on the MOC 7 and EOC 7 (before outage for thermal shield support repair).

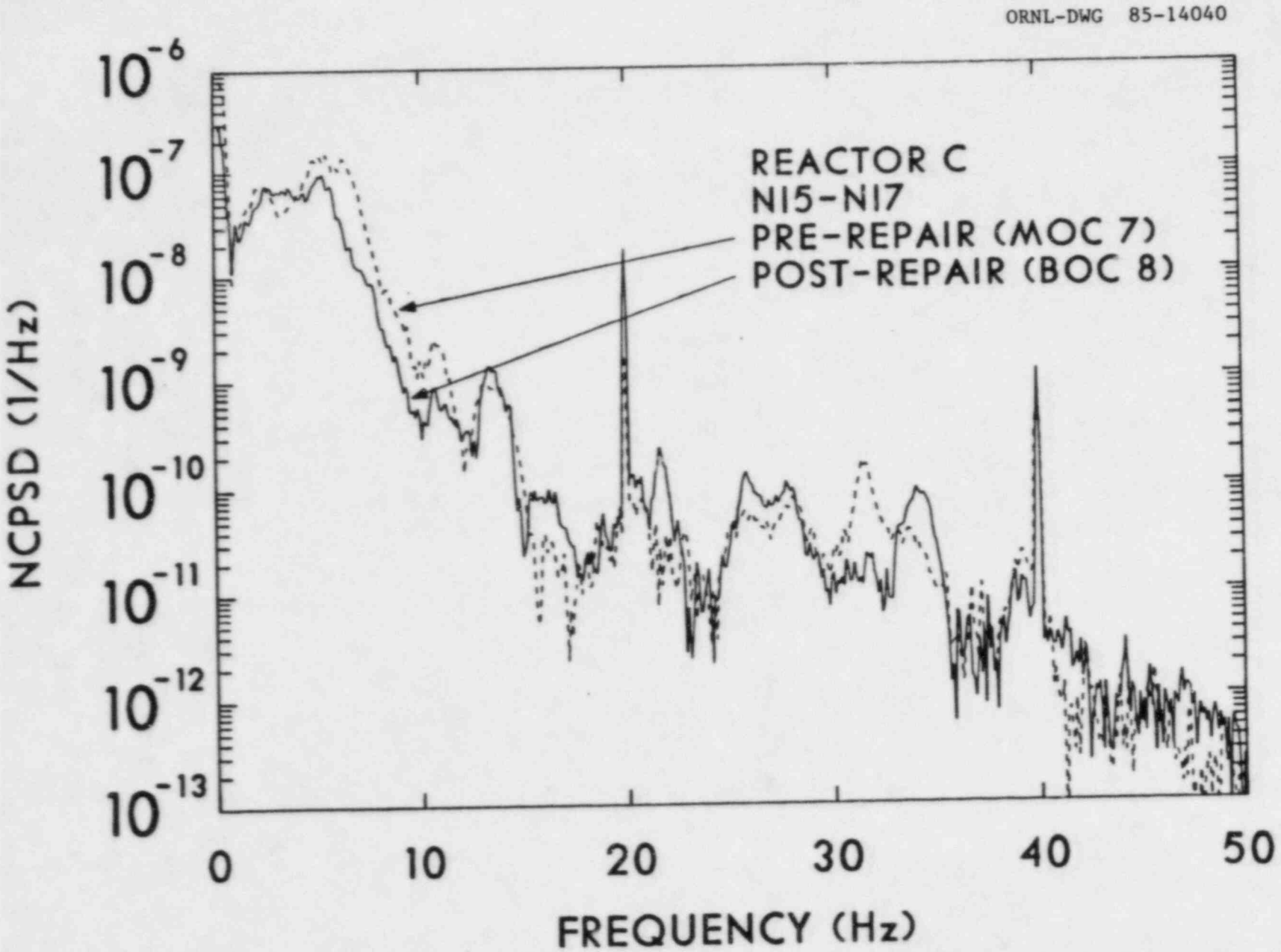

Fig. 7.12. Comparison between NCPSDs for cross-core detector pair NI 5 and NI 7 at Reactor C before (MOC 7) and after (BOC 8) repair of thermal shield supports.

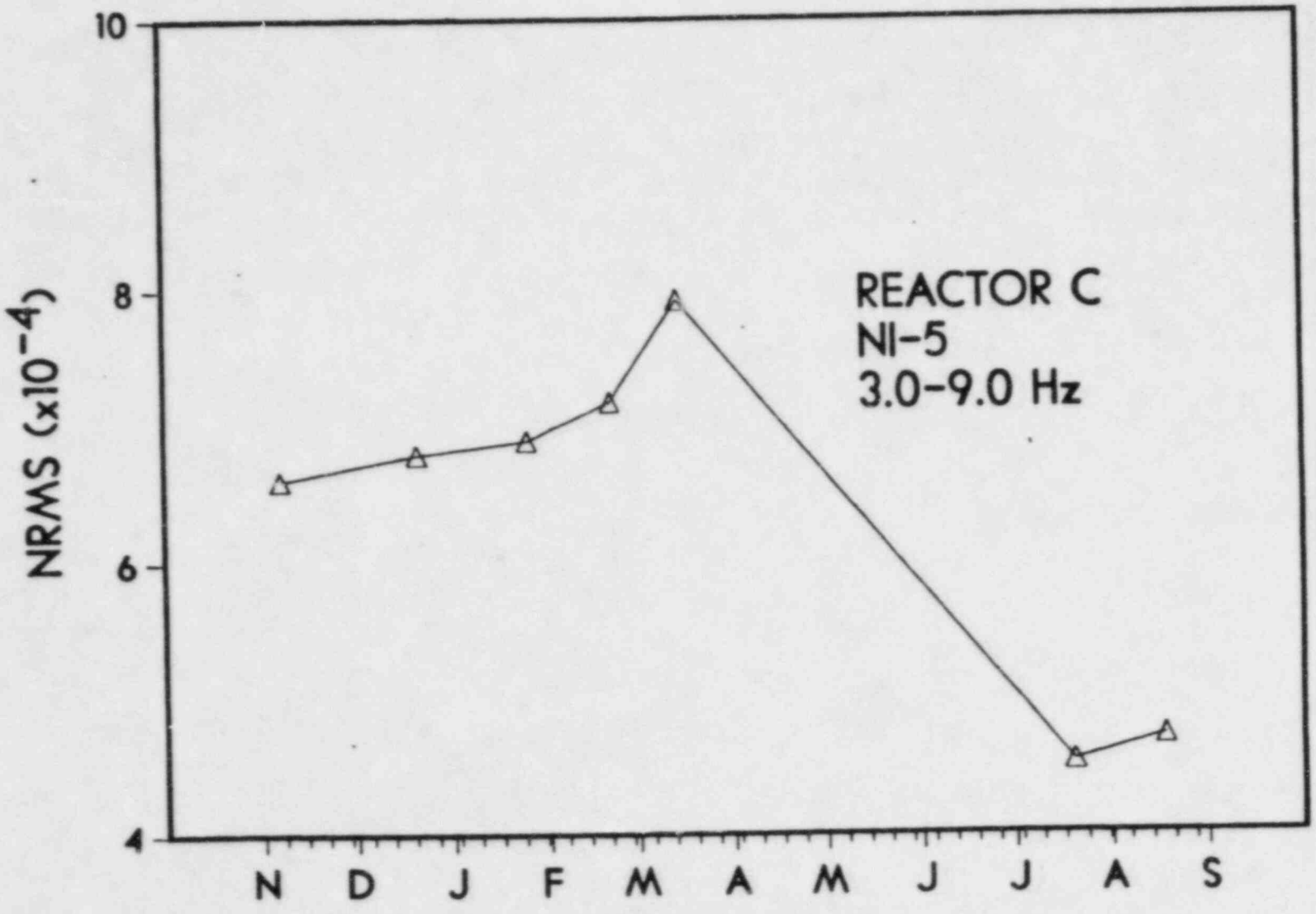

Fig. 7.13. Normalized root mean square (NRMS) over 3-9 Hz versus time for detector NI 5 at Reactor C.

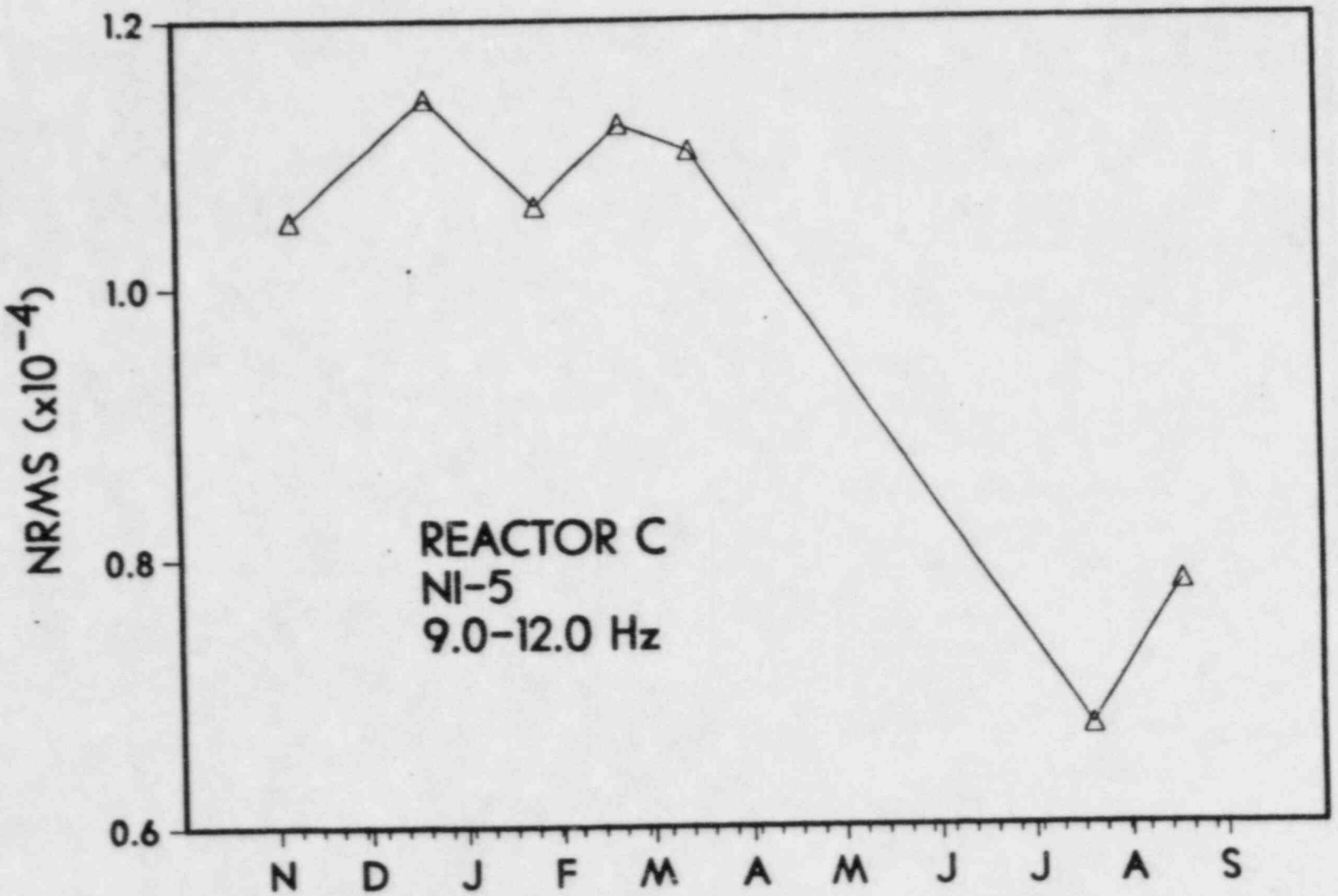

Fig. 7.14. NRMS over 9-12 Hz versus time for detector NI 5 at Reactor C.

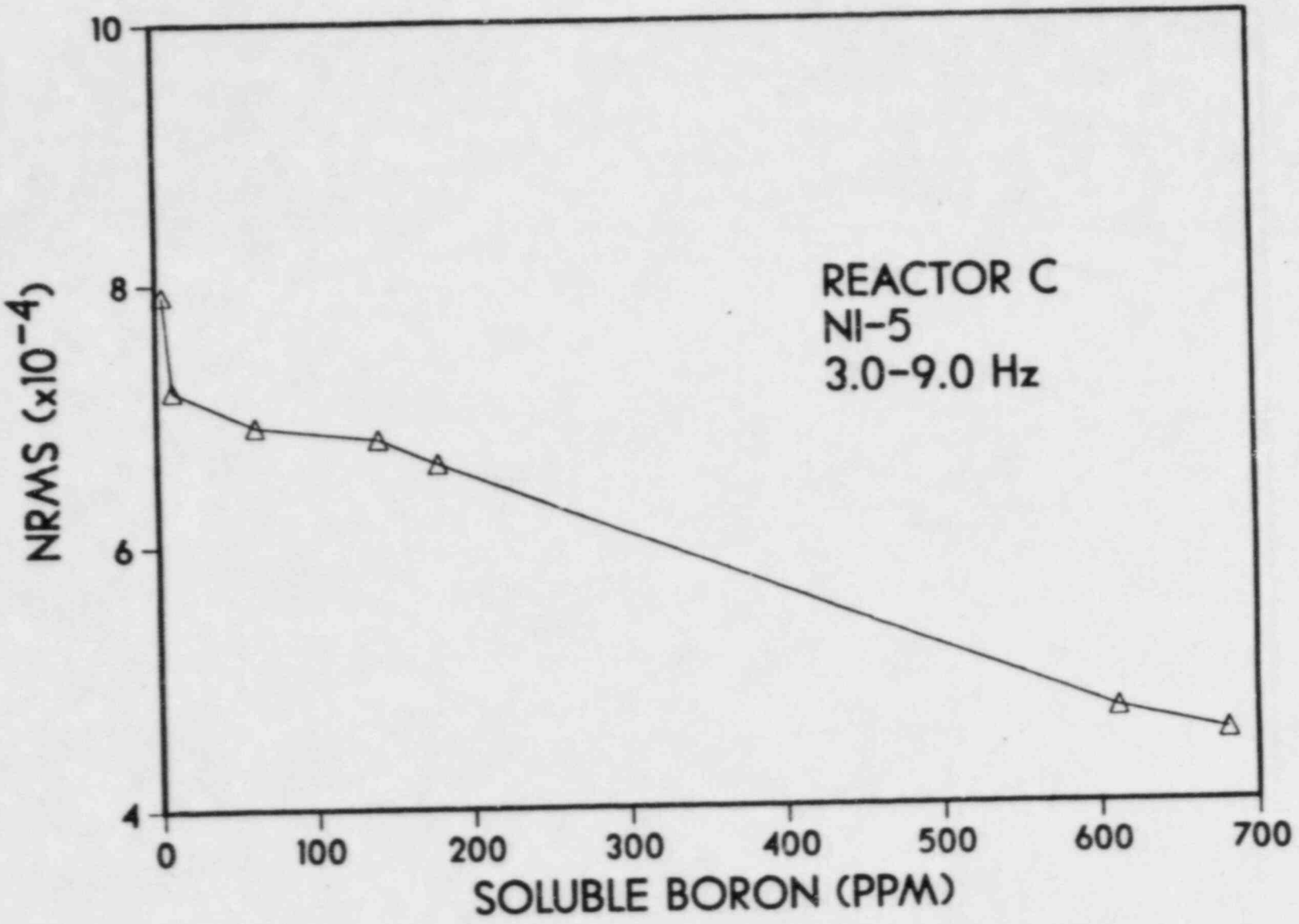

Fig. 7.15. NRMS over 3-9 Hz versus soluble boron concentration at Reactor C.

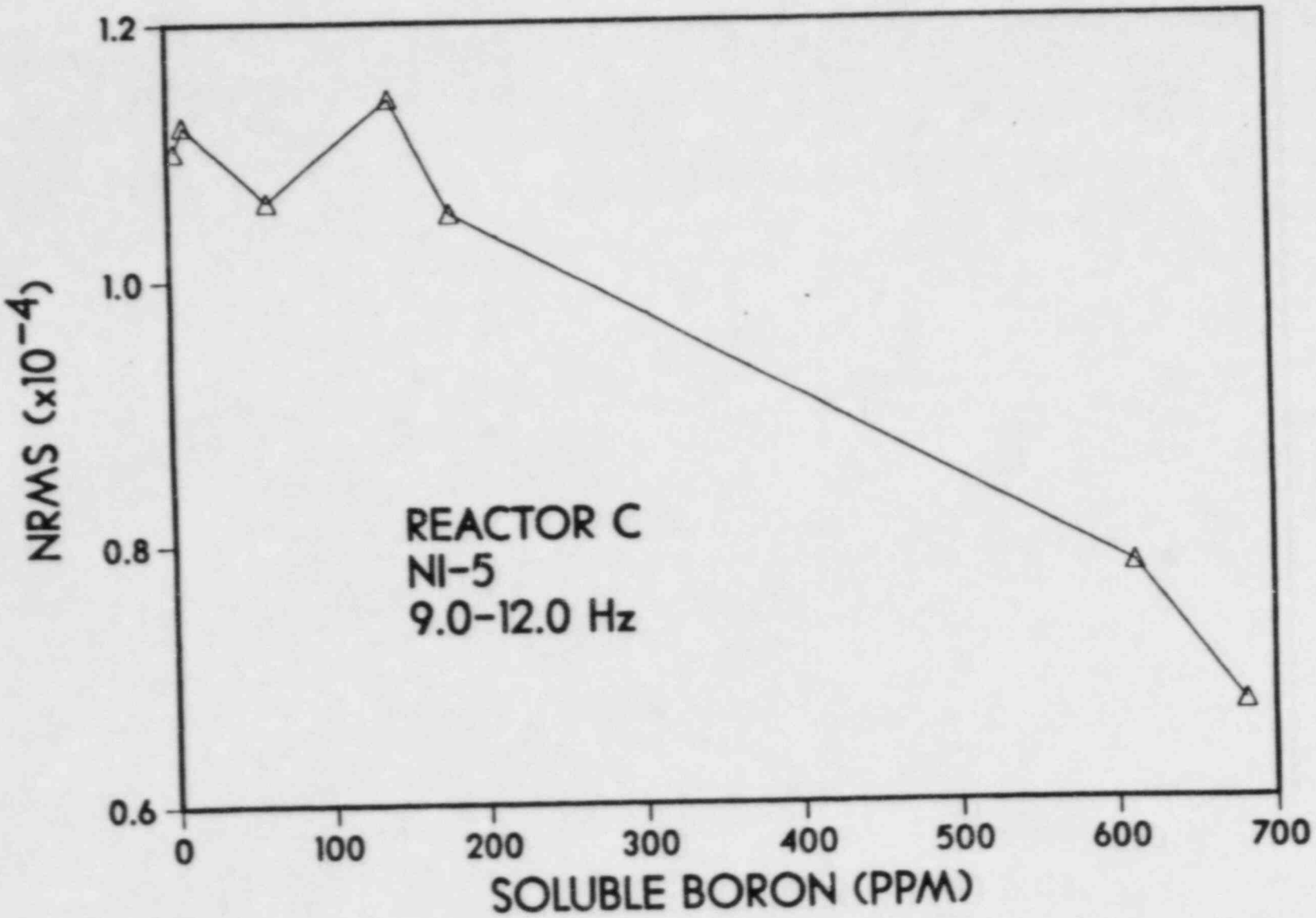

Fig. 7.16. NRMS over 9-12 Hz versus soluble boron concentration at Reactor C.

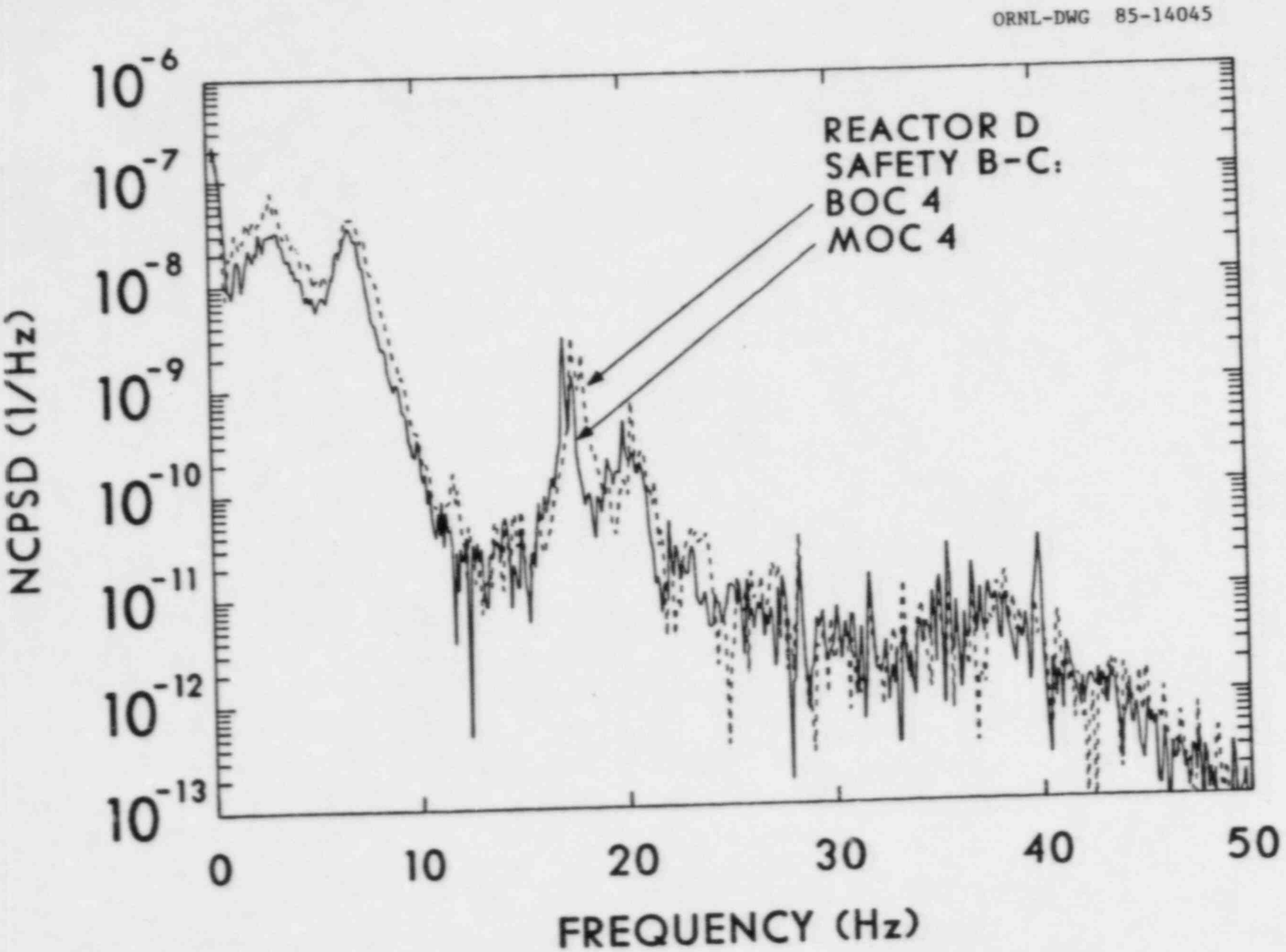

Fig. 7.17. NCPSDs for cross-core detector pair Safety B and Safety C at Reactor D on the BOC 4 and MOC 4.

NRMS values over the 5- to 10- and 15- to 19-Hz frequency ranges (Figs. 7.18 and 7.19 respectively) showed generally decreasing trends with time. Without additional data, it is not possible to determine if these trends are related to burnup.

7.5 INTERPLANT COMPARISON

Because of structural similarities (especially size) and the existence of thermal shield damage, we compared the results of Reactor A with Reactor B. We also compared Reactor B noise data obtained after removal of the thermal shield with data from Calvert Cliffs-1, an 830 MW(e), 2-loop, CE plant without a thermal shield. The Calvert Cliffs-1 data were obtained through the NRC's baseline noise program (FIN B0191).

Figure 7.20 compares cross-core detector NCPSDs from Reactors A and B at the BOC5 which preceded discovery of thermal shield damage. As was discussed in Sect. 5, we postulate that the two orders of magnitude difference between the two spectra is due to incorrect normalization of the Reactor B data. From this comparison, however, it can be seen that the resonant frequency associated with pendular CSB motion is higher for Reactor A (7.5 Hz) than for Reactor B (7 Hz). The resonance associated with shell-mode vibrations is lower in frequency for Reactor A (13 Hz) and sharper compared to Reactor B (14.5 Hz). A low-frequency resonance occurs in the Reactor A data at 1.5 Hz which is not visible in the Reactor B data. Comparison of the coherences from the two plants (Fig. 7.21) also shows this behavior. In addition, coherences >0.4 can be seen in the 12- to 16- and 17- to 21-Hz ranges. As was shown in the Reactor B data, cross-core detector coherences changed significantly in the 10- to 20-Hz range when the thermal shield was removed. Figure 7.22 shows a comparison of the cross-core detector coherences between Calvert Cliffs-1 and Reactor B without its thermal shield. The coherences are similar below 25 Hz, although the Reactor B and Calvert Cliffs data exhibit slight differences in the 12- to 15-Hz range.

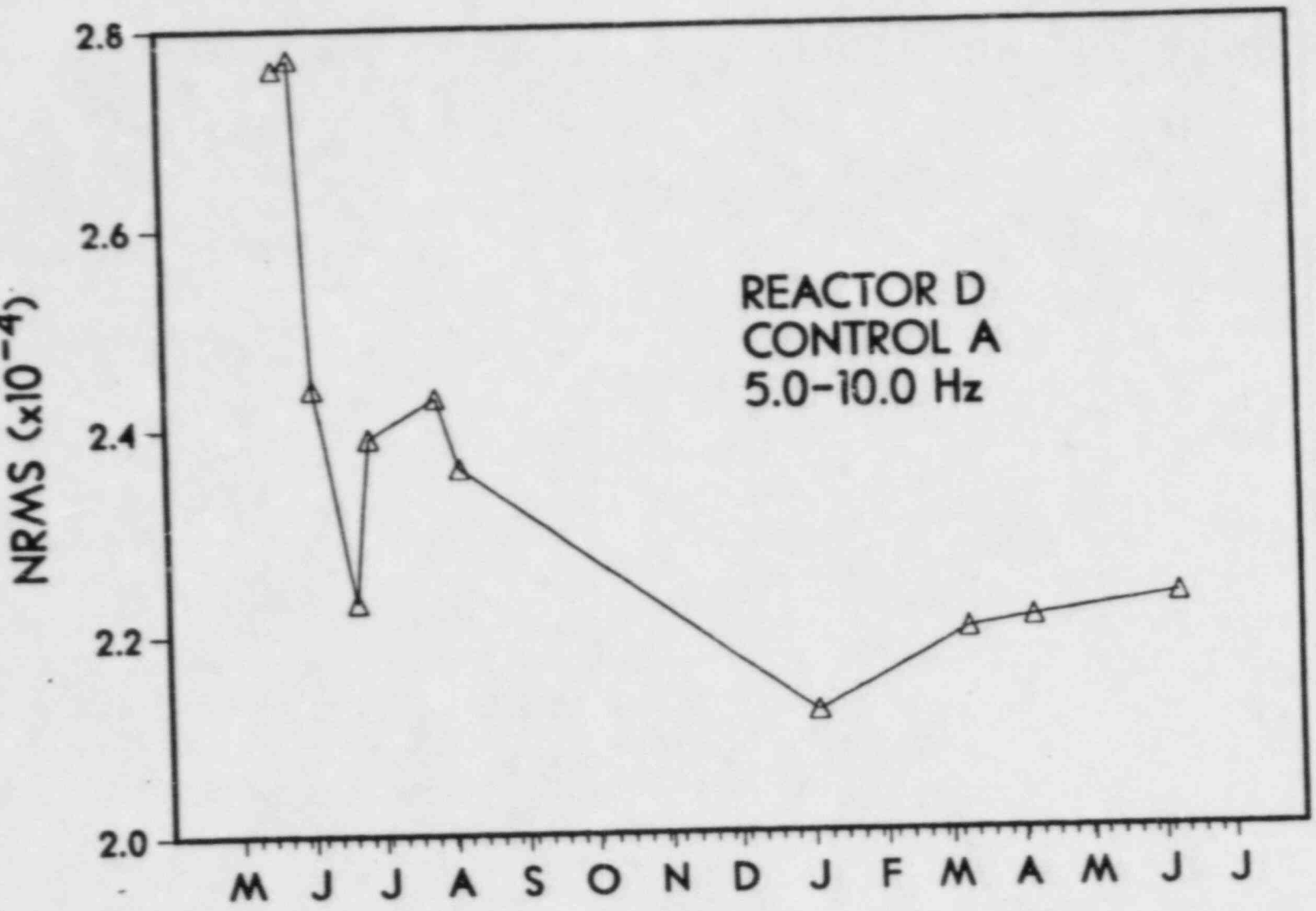

Fig. 7.18. NRMS over 5-10 Hz versus time for detector Control A at Reactor D.

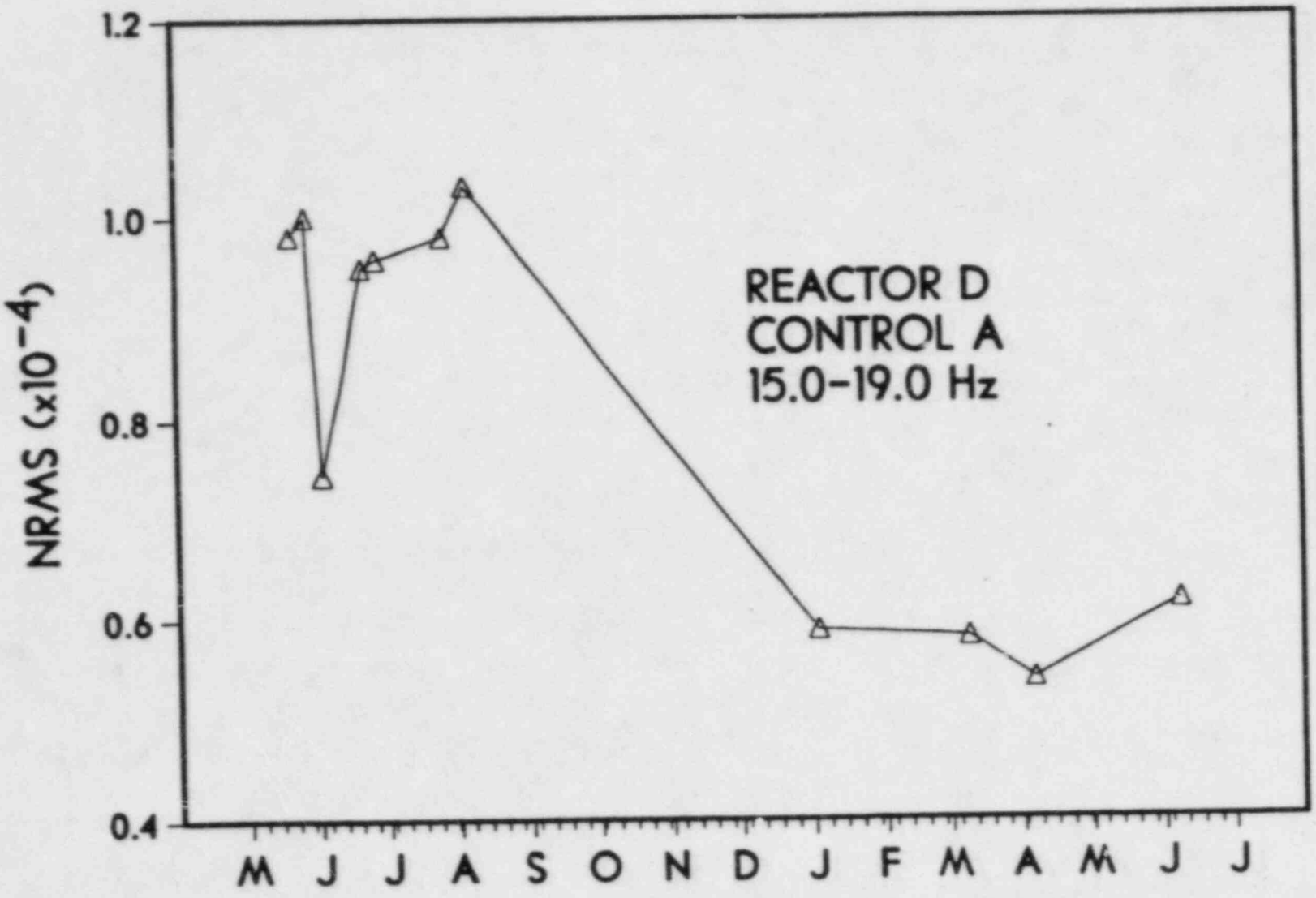

Fig. 7.19. NRMS over 15-19 Hz versus time for detector Control A at Reactor D.

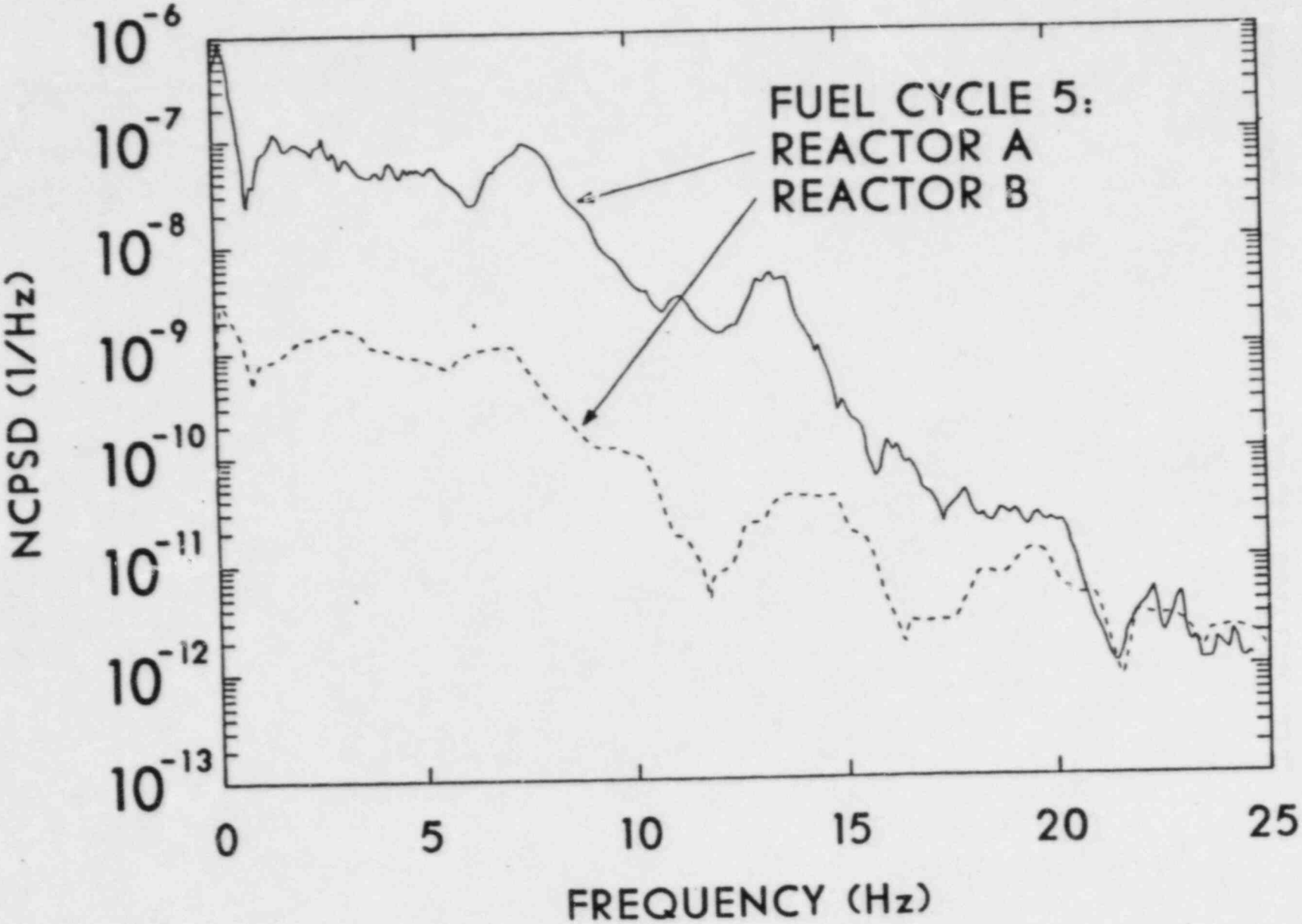

Fig. 7.20. Comparison of cross-core NCPSDs at Reactor A and Reactor B at BOC 5 (prior to the thermal shield removal).

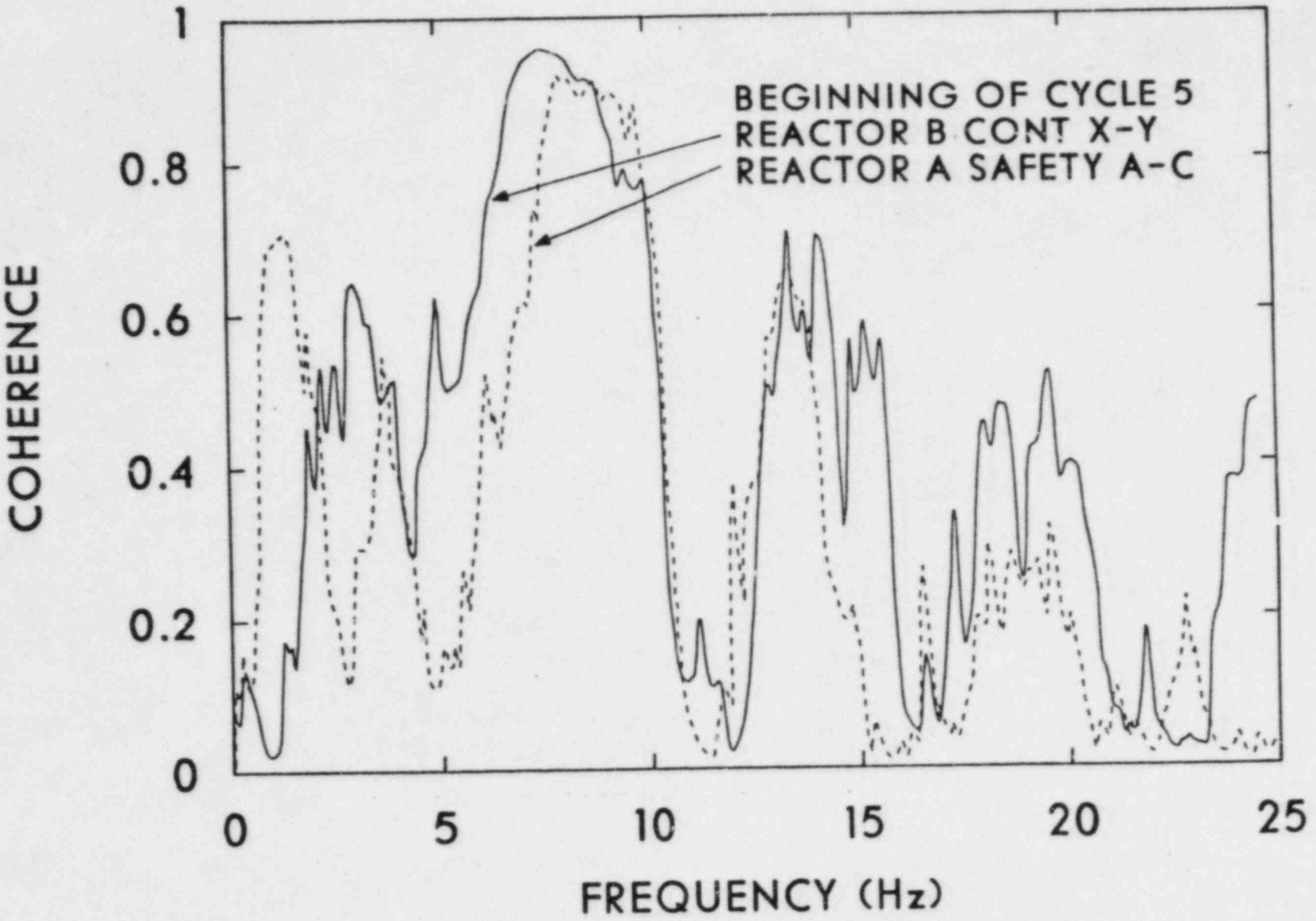

Fig. 7.21. Comparison of cross-core detector coherence from Reactor A and Reactor B at BOC 5 (prior to the thermal shield removal).

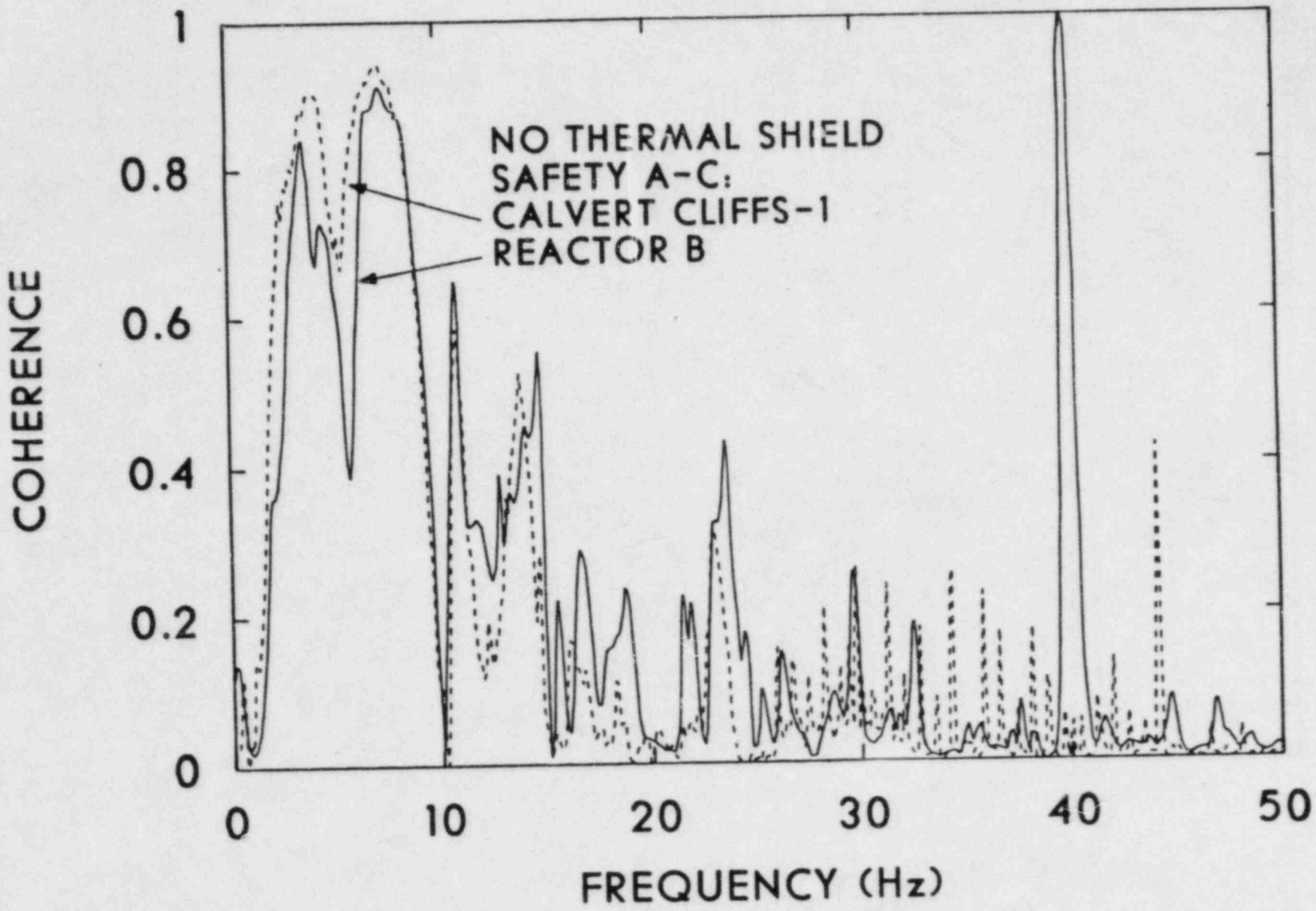

Fig. 7.22. Comparison of cross-core detector coherences from Reactor B (thermal shield removed) and Calvert Cliffs-1 (constructed without a thermal shield).

7.6. INTERPRETATION OF DATA

Based on the previously discussed observations and calculations, and our experience with the behavior of neutron noise in other plants, we made the following interpretations:

1. Reactor A and Reactor B neutron noise data exhibit frequency shifts in the resonances associated with CSB, thermal shield, and fuel assembly structures.
2. These changes are abnormal when compared to other plants, with or without thermal shields over a fuel cycle; specifically, Sequoyah[2] and Calvert Cliffs.[7]
3. The observed trends in the experimental data (increasing CSB beam mode frequency and decreasing shell mode frequencies) are predicted by finite element model calculations when degraded thermal shield supports are assumed.
4. Reactor A exhibited larger changes in resonant frequencies than Reactor B indicating a greater change in structural dynamics prior to discovery of thermal shield damage.
5. Reactor A data exhibit a low frequency resonance which may be the result of decoupled CSB and thermal shield motions. Since thermal shield vibrations are unlikely to directly increase neutron noise, this resonance might be the result of thermal shield impacting on the CSB.
6. Reactor B data exhibit growth in cross-core detector coherences at two shell mode frequencies indicating increased stimulation of CSB/thermal shield resonances or a significant change in their preferential direction of vibration.
7. The greatest changes in resonant frequencies or detector coherences occurred during the first or second fuel cycle of both Reactor A and Reactor B. Therefore, we hypothesize that loosening of the thermal shield supports occurred early in plant life in both cases.

8. When the thermal shield was removed from Reactor B, the noise signatures became similar to those from Calvert Cliffs-1, a plant constructed without a thermal shield.
9. We believe that the small amount of data (<1 fuel cycle) from Reactor C and Reactor D is inadequate to confirm or deny problems in the CSB or thermal shield supports at these plants. Comparison would have to be made with data taken early in plant life. Furthermore, we believe there is insufficient evidence from Reactor C to indicate that the changes in neutron noise observed after thermal shield support repair are solely attributable to that repair.

8. CONCLUSIONS AND RECOMMENDATIONS

As a result of this study, the following conclusions are drawn:

1. Thermal shield support degradation at Reactors A and B manifested itself in the ex-core neutron noise spectra.
2. The degradation was apparent from changes in frequency of structural vibration resonances or changes in cross-core detector coherence.
3. The observed frequency changes in the neutron noise resonances of Reactors A and B were similar to those predicted by finite element structural models of degraded thermal shield supports.
4. Degradation of thermal shield supports at Reactors A and B probably started early in plant life.

As a result of this study we make the following recommendations for early detection of thermal shield support degradation:

1. Surveillance of the ex-core neutron noise should cover the 0- to 50-Hz frequency range.
2. Four ex-core detectors, positioned approximately 90° apart, should be analyzed, including NCPSDs for all combinations of detector pairs (both cross-core and adjacent).
3. Upper and lower half detectors should be analyzed separately, since both experimental and calculated data show an axial dependence of internal vibrations.
4. Interpretation of neutron noise should emphasize the frequency of resonances, and surveillance should be performed for changes in these frequencies.
5. Statistically significant changes or trends in the ex-core neutron noise, particularly changes in the frequency of a resonance, should be considered abnormal until the cause of the change has been identified.

6. Ex-core neutron noise should be supplemented with accelerometer measurements since changes in the neutron noise amplitude may be difficult to interpret. Such measurements would ideally be independent of a loose parts monitoring system (LPMS) and may require optimal sensor location (i.e., the pressure vessel head flange).
7. Surveillance of the ex-core neutron noise should be performed periodically: a minimum of once every three months with monthly surveillance being preferred.
8. Plants should have a calibrated and operating LPMS. Changes in the neutron noise, preceding or existing with impacts detected by the LPMS, indicate the need for immediate diagnostic action. A LPMS alone may not be adequate for core internals surveillance, since significant structural degradation may have already occurred by the time impacts cause an LPMS alarm.

As a consequence of the data deficiencies observed in this study, we also make the following recommendations for a noise surveillance program:

1. Data acquisition, analysis, and interpretation should be performed by personnel trained and experienced in neutron noise analysis.
2. QA procedures should be developed to ensure that data acquisition and analysis activities are performed correctly and adequately documented.
3. Noise analysis results should be displayed using consistent plot size and scales.
4. Preferred units for NPSD or NCPSD are volts^2/(unit volt dc)^2/(unit gain)/Hz (i.e., 1/Hz).
5. Enough data should be acquired to ensure a high degree of statistical confidence in the noise analysis results. Typically, this would require a minimum of 100 data block averages (no overlap processing) with a minimum sample blocksize of 1024 and spanning the 0- to 50-Hz frequency range (a minimum of 18 min of data with 30 min of data preferred).

9. ADDITIONAL WORK NEEDED

As a result of this study, the following areas were identified for additional work that would improve the application and interpretation of neutron noise analysis for monitoring the condition of core intervals:

- In-core neutron noise: Fuel assembly vibrations have been found to contribute to ex-core neutron noise at frequencies below 50 Hz. This contribution complicates interpretation of changes in ex-core neutron noise. The long term behavior of in-core neutron noise and its contribution to ex-core neutron noise should be studied from both experimental and theoretical aspects.

- Internals aging and structural interactions: Postulated degradation of reactor internals due to aging and the resulting effects on the neutron noise should be studied. Such studies would include experimental measurements of how structural vibrations interact to produce neutron noise.

- Operational and Reactor Physics Effects: Ex-core neutron noise is dependent on thermal-hydraulic and reactor physics (burnup, soluble boron, etc.) conditions in the reactor. The dependence of the neutron noise on these factors should be studied in order to improve interpretation of changes in noise amplitude.

- Reactor A: Neutron noise data should be acquired after removal of the thermal shield and compared with other plants operating without thermal shields.

- Reactor C: Neutron noise data acquisition should be continued. Sources of changes in noise amplitude should be determined.

- Reactor D: Source of ~17-Hz resonance in the neutron noise should be identified.

REFERENCES

1. P. Bernard, et al., "Quantitative Monitoring and Diagnosis of French PWRs' Internal Structures Vibrations by Ex-Core Neutron Noise and Accelerometers Analysis," Prog. Nucl. Energy 9, 465-492 (1982).

2. F. J. Sweeney, J. March-Leuba, C. M. Smith, "Contribution of Fuel Vibrations to Ex-Core Neutron Noise During the First and Second Fuel Cycles of the Sequoyah-1 Pressurized Water Reactor," Proc. Fourth Specialists' Meeting on Reactor Noise (SMORN-IV), October 15-19, 1984, Dijon, France.

3. D. N. Fry, J. March-Leuba, F. J. Sweeney, Use of Neutron Noise for Diagnosis of In-Vessel Anomalies in Light-Water Reactors, NUREG/CR-3303 (ORNL/TM-8774), Oak Ridge National Laboratory (1984).

4. PAFEC 75 Data Preparation, PAFEC, Ltd., Nottingham, England, November 1978.

5. F. J. Sweeney, "Interim Report: Detection of Core-Barrel Motion and Thermal-Shield Vibrations Using Ex-Core Neutron Noise," letter report to N. N. Kondic (NRC Division of Facility Operations, FIN B0191) and L. L. Lois (NRC Division of Systems Integration, FIN B0777) October 1983.

6. W. Bastl and D. Wach, "Experiences with Noise Surveillance Systems in German LWRs," Prog. Nucl. Energy 9, 505-516 (1982).

7. J. P. Steelman and B. T. Lubin, "Analysis of Changes with Operating Time in the Calvert Cliffs Unit 1 Noise Signals," Prog. Nucl. Energy 1, 379-391 (1977).